Electronic Supplementary Material (ESI) for ChemComm.

Supporting Information

Structural Diversity in Multinuclear Tantalum Polyhydrides Formed via Reductive Hydrogenolysis of Metal-Carbon Bonds

*Jade I. Fostvedt, Trevor D. Lohrey, Robert G. Bergman, and John Arnold**

Department of Chemistry, University of California, Berkeley, CA, 94720, United States

Table of Contents

A. Experimental Section

General Considerations. Unless otherwise stated, all reactions were performed under an atmosphere of dry N_2 using standard Schlenk line techniques or in an MBraun inert atmosphere glovebox under an atmosphere of nitrogen (<1.0 ppm O_2/H_2O). All glassware, cannulae, and Celite were stored in an oven at ca. 150 °C for at least 12 h prior to use. Molecular sieves (4 Å) were activated by heating to 200 °C overnight under vacuum and then stored in a glovebox. NMR spectra were obtained at ambient temperature, unless otherwise noted, using Bruker AVB-400, AV-500, DRX-500, and AV-600 spectrometers. ^1H and $^{13}C\{^1H\}$ NMR chemical shifts (δ) were reported relative to residual solvent peaks. $^{11}B\{^1H\}$ NMR chemical shifts (δ) were referenced to an external standard ($BF_3{\cdot}OEt_2$). ^1H and ^{13}C NMR assignments were routinely confirmed by ^1H-^{13}C HSQC NMR experiments. Fourier transform infrared (FT-IR) samples were prepared as Nujol mulls and were taken between KBr disks using a Nicolet iS10 FT-IR spectrometer. Melting points were determined using an Optimelt SRS automated melting point system using sealed capillaries prepared under an atmosphere of dry N_2. Elemental analysis samples were sealed under vacuum in ampules and analyzed at the London Metropolitan University.

Materials. Diethyl ether (Et_2O), *n*-hexane, toluene, benzene, and tetrahydrofuran (THF) were dried and degassed using a Phoenix solvent drying system commercially available from JC Meyer Solvent Systems. THF-d_8, toluene-d_8, and C_6D_6 were obtained from Cambridge Isotope Laboratories and dried using sodium/benzophenone, degassed with three freeze-pump-thaw cycles, and vacuum-transferred or distilled prior to storage in a glovebox over molecular sieves. *N*-Mesitylimidazole,[1] $[H_2B(^{Mes}ImH)_2][I]$,[2] $[H_2B(^{Mes}ImH)_2][Cl]$,[3] lithium diisopropylamide (LDA),[4] $TaMe_3Cl_2$,[5] and KC_8[6] were prepared according to literature procedures. All other reagents were acquired from commercial sources and used as received.

Synthetic Procedures.

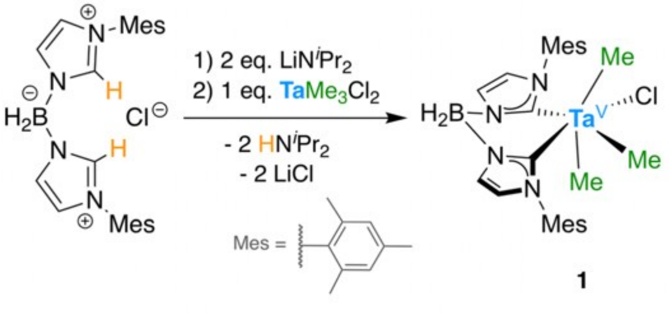

Scheme S1. Synthesis of **1**.

$[H_2B(^{Mes}Im)_2]TaMe_3Cl$ (1). $[H_2B(^{Mes}ImH)_2][Cl]$ (3.22 g, 7.65 mmol) and LDA (1.64 g, 15.3 mmol) were combined in a 250 mL round-bottomed Schlenk flask and cooled to –78 °C. THF (100 mL) was cooled to –78 °C and added to the solid mixture, and the off-white suspension was warmed to 0 °C and stirred for 1 h. The peach-colored reaction mixture was again cooled to –78 °C. In another 250 mL round-bottomed Schlenk flask, a solution of $TaMe_3Cl_2$ (2.0 g, 7.65 mmol) in THF (50 mL) was cooled to –78 °C, resulting in a bright yellow solution. The peach solution was added to the yellow solution via a cannula, resulting in a color change to dark orange. The solution was warmed to 0 °C and stirred for 3 h, resulting in a dark red solution. The volatile materials were removed under vacuum, and the resulting yellow oil was triturated with hexane (2 × 20 mL), affording a yellow powder. The powder was extracted with toluene (3 × 30 mL), and the combined extracts were filtered through Celite and concentrated to ca. 45 mL. The solution was stored at –40 °C overnight, yielding golden-yellow crystals of **1** (3.57 g, 72% yield; the molecular mass was calculated to include one equivalent of toluene solvent, as observed by ^1H NMR spectroscopy). X-ray quality crystals of **1** were grown from a saturated solution of **1** in toluene at –40 °C. Mp 143 °C (decomp). ^1H NMR (400 MHz, C_6D_6) $\delta = 6.78$ (d, $J = 1.5$ Hz, HC_{Imid}, 2H), 6.59 (s, HC_{Mes}, 4H), 6.02 (d, $J = 1.5$ Hz, HC_{Imid}, 2H), 3.51 (br s, HB, 2H), 1.97 (s, H_3C_{Mes}, 18H), 1.35 (br s, TaMe_3, 9H). ^{13}C NMR (101 MHz, C_6D_6) $\delta = 138.7$, 135.7, 135.5, 129.1 (HC_{Mes}), 123.8 (HC_{Imid}), 121.9 (HC_{Imid}), 20.9 (H_3C_{Mes}), 19.0 (H_3C_{Mes}). ^{11}B NMR (193 MHz, C_6D_6) $\delta = -13.74$. FT-IR (KBr, Nujol, cm^{-1}) 2456 (m, $\nu_{\mathrm{B-H}}$), 2360 (m, $\nu_{\mathrm{B-H}}$), 2167 (m, $\nu_{\mathrm{B-H}}$), 2128 (m, $\nu_{\mathrm{B-H}}$). Anal. calcd for $C_{27}H_{37}BN_4ClTa$ (**1**): C, 50.29; H, 5.78; N, 8.69. Found: C, 50.31; H, 5.82; N, 8.74.

$[H_2B(^{\mathrm{Mes}}Im)_2]TaMe_4$ (2). Compound **1·toluene** (2.06 g, 2.79 mmol) was dissolved in Et_2O (150 mL) in a 250 mL round-bottomed Schlenk flask. The bright yellow solution was cooled to –78 °C, and methyllithium (1.6 M, 1.74 mL, 2.79 mmol) was added dropwise via syringe. The solution was warmed to 0 °C and stirred for 1 h, resulting in a cloudy, pale yellow solution. The volatile materials were removed under vacuum, and the pale yellow solids were triturated with hexane (2 × 25 mL), resulting in a cream-colored powder. The powder was extracted with toluene (3 × 20 mL), and the combined extracts were filtered through Celite and concentrated to ca. 2 mL. The amber-colored solution was stored at –40 °C overnight, yielding pale yellow crystals of **2** (1.67 g, 84% yield; the molecular mass was calculated to include one equivalent of toluene solvent, as observed by ^1H NMR spectroscopy). X-ray quality crystals of **2·toluene** were grown by vapor diffusion of hexane into a saturated toluene solution of **2** at room temperature. Mp 63 °C (decomp). ^1H NMR (600 MHz, toluene-d_8) $\delta = 6.81$ (d, $J = 1.0$ Hz, HC_{Imid}, 2H), 6.63 (s, HC_{Mes}, 2H), 6.60 (s, HC_{Mes}, 2H), 6.10 (d, $J = 0.9$ Hz, HC_{Imid}, 2H), 3.42 (br m, HB, 2H), 2.08 (s, H_3C_{Mes}, 6H, overlaps toluene-d_8 peak), 2.00 (s, H_3C_{Mes}, 6H), 1.77 (s, H_3C_{Mes}, 6H), 1.10 (br s, TaMe_4, 12H). ^{13}C NMR (151 MHz, toluene-d_8) $\delta = 204.6$ (C_{Imid}), 138.3, 136.3, 129.4 (HC_{Mes}), 129.2 (HC_{Mes}), 128.6, 128.2, 125.4 (HC_{Imid}), 123.8 (HC_{Imid}), 121.5 (HC_{Imid}), 20.8 (H_3C_{Mes}), 18.8 (H_3C_{Mes}). ^{11}B NMR (193 MHz, toluene-d_8) $\delta = -14.49$. FT-IR (KBr, Nujol, cm^{-1}) 2437 (m, $\nu_{\mathrm{B-H}}$), 2294 (w, $\nu_{\mathrm{B-H}}$), 2117 (m, $\nu_{\mathrm{B-H}}$), 2046 (m, $\nu_{\mathrm{B-H}}$). Anal. calcd for $C_{28}H_{42}BN_4Ta$ (**2**): C, 53.69; H, 6.76; N, 8.94. Found: C, 53.53; H, 6.59; N, 8.94.

$\{[H_2B(^{\mathrm{Mes}}Im)_2]TaCl\}_2(\mu\text{-}H)_4$ (3). Compound **1·toluene** (1.0 g, 1.36 mmol) was added to a 250 mL round-bottomed Schlenk flask and dissolved in benzene (25 mL). The solution was degassed, and the headspace was refilled with H_2. The solution immediately changed color from bright yellow to dark red. The flask was sealed, and the solution was stirred vigorously at ambient temperature for 24 h; over the course of the reaction, the solution progressed in color from dark red to dark reddish-brown. The volatiles were removed via lyophilization, affording a dark brown powder. The crude product was extracted with toluene (3 × 30 mL), and the combined extracts were filtered through Celite, concentrated to ca. 20 mL, and stored at –40 °C overnight, yielding dark burgundy crystals of **3** (658 mg, 75% yield; the molecular mass was calculated to include one equivalent of toluene solvent, as observed by ^{1}H NMR spectroscopy). X-ray quality crystals of **3·toluene** were grown by vapor diffusion of hexane into a saturated toluene solution of **3** at room temperature. Mp 166 °C (decomp). ^{1}H NMR (600 MHz, C_6D_6) δ = 7.30 (br s, $H\mathrm{C}_{\mathrm{Imid}}$, 2H), 7.25 (br s, $H\mathrm{C}_{\mathrm{Imid}}$, 2H), 7.11 (br s, $H\mathrm{C}_{\mathrm{Mes}}$, 2H, overlaps toluene peak), 6.91 (br s, $H\mathrm{C}_{\mathrm{Mes}}$, 2H), 6.64 (s, $H\mathrm{C}_{\mathrm{Mes}}$, 4H), 6.21 (br s, $H\mathrm{C}_{\mathrm{Imid}}$, 4H), 4.48 (br s, *H*B, 4H), 2.18 (br s, $H_3\mathrm{C}_{\mathrm{Mes}}$, 3H), 2.14 (br s, $H_3\mathrm{C}_{\mathrm{Mes}}$, 3H), 2.07 (br s, $H_3\mathrm{C}_{\mathrm{Mes}}$, 3H), 2.05 (br s, $H_3\mathrm{C}_{\mathrm{Mes}}$, 3H), 2.01 (br s, $H_3\mathrm{C}_{\mathrm{Mes}}$, 6H), 1.85 (br s, $H_3\mathrm{C}_{\mathrm{Mes}}$, 6H), 1.72 (br s, $H_3\mathrm{C}_{\mathrm{Mes}}$, 6H), 1.60 (br s, $H_3\mathrm{C}_{\mathrm{Mes}}$, 6H). ^{13}C and ^{11}B NMR spectroscopic data were not obtained due to the broadness of the signals at room temperature. FT-IR (KBr, Nujol, cm^{-1}) 2395 (m, $\nu_{\mathrm{B\text{-}H}}$), 2359 (m, $\nu_{\mathrm{B\text{-}H}}$). Anal. calcd for $C_{48}H_{64}B_2Cl_2N_8Ta_2$ (**3**): C, 47.75; H, 5.34; N, 9.28. Found: C, 47.99; H, 5.24; N, 9.13.

{[H$_2$B($^{\mathrm{Mes}}$Im)$_2$]TaCl}$_2$(μ-D)$_4$ (3-*d*$_4$). Compound **1·toluene** (187 mg, 0.254 mmol) was added to a 250 mL round-bottomed Schlenk flask and dissolved in benzene (10 mL). The solution was degassed, and the headspace was refilled with D_2. After five minutes, the solution changed color from bright yellow to dark red. The flask was sealed, and the solution was stirred vigorously at ambient temperature for 5 days; over the course of the reaction, the solution progressed in color from dark red to dark reddish-brown. The volatiles were removed via lyophilization, affording a dark brown powder. The crude product was extracted with boiling toluene (3 × 5 mL), and the combined extracts were filtered through Celite, concentrated to ca. 5 mL, and stored at –40 °C overnight, yielding dark burgundy crystals of **3-*d*$_4$** (87.1 mg, 53% yield; the molecular mass was calculated to include one equivalent of toluene solvent, as observed by ^{1}H NMR spectroscopy). ^{1}H NMR (600 MHz, toluene-*d*$_8$) δ = 7.25 (br s, $H\mathrm{C}_{\mathrm{Imid}}$, 2H), 7.18 ($H\mathrm{C}_{\mathrm{Imid}}$, 2H), 6.89 (br s, $H\mathrm{C}_{\mathrm{Mes}}$, 4H), 6.60 (br s, $H\mathrm{C}_{\mathrm{Mes}}$, 4H), 6.22 (br s, $H\mathrm{C}_{\mathrm{Imid}}$, 2H), 6.19 (br s, $H\mathrm{C}_{\mathrm{Imid}}$, 2H), 4.33 (br s, *H*B, 4H), 2.21 (br s, $H_3\mathrm{C}_{\mathrm{Mes}}$, 6H), 2.10 (br s, $H_3\mathrm{C}_{\mathrm{Mes}}$, 6H), 1.94 (br s, $H_3\mathrm{C}_{\mathrm{Mes}}$, 6H), 1.93 (br s, $H_3\mathrm{C}_{\mathrm{Mes}}$, 6H), 1.68 (br s, $H_3\mathrm{C}_{\mathrm{Mes}}$, 6H), 1.55 (br s, $H_3\mathrm{C}_{\mathrm{Mes}}$, 6H). ^{2}H NMR (92 MHz, toluene) δ = 11.54 (br s, *μ-D*, 4D). ^{13}C and ^{11}B NMR data were not obtained due to the broadness of the signals at room temperature. FT-IR (KBr, Nujol, cm^{-1}) 2394 (m, $\nu_{\mathrm{B\text{-}H}}$), 2359 (m, $\nu_{\mathrm{B\text{-}H}}$).

{[H$_2$B($^{\mathrm{Mes}}$Im)$_2$]Ta}$_2$(μ-H)$_2$(μ-η^4:η^4-C$_6$H$_6$) (4).

Method A. Compound **2·toluene** (500 mg, 0.696 mmol) was added to a 250 mL round-bottomed Schlenk flask and dissolved in benzene (20 mL). The solution was degassed, and the headspace was refilled with H_2. After 15 minutes, the solution changed color from bright yellow to orange. The flask was sealed, and the solution was stirred vigorously at ambient temperature for 24 h. Then, the H_2 was removed, the solution was degassed, and the headspace was refilled with N_2. The solution was stirred vigorously at ambient temperature for an additional 48 h. Over the course of the reaction, the solution progressed in color from orange to dark purple. The volatiles were removed via lyophilization, resulting in a dark purple powder. The crude product was extracted with toluene (3 × 8 mL), and the resulting solution was filtered through Celite, concentrated to a final volume of ca. 2 mL, and stored at –40 °C overnight, yielding dark blue crystals of **4** (372 mg, 77% yield; the molecular mass was calculated to include two equivalents of toluene solvent, as observed by ^{1}H NMR spectroscopy). X-ray quality crystals of **4** were grown by vapor diffusion of hexane into a saturated toluene solution of **4** at room temperature. Mp 189

°C (decomp). ^{1}H NMR (600 MHz, toluene-*d*$_8$) δ = 6.86 (d, *J* = 1.6 Hz, *H*C$_{\text{Imid}}$, 4H), 6.69 (s, *H*C$_{\text{Mes}}$, 4H), 6.61 (s, *H*C$_{\text{Mes}}$, 4H), 6.10 (d, *J* = 1.6 Hz, *H*C$_{\text{Imid}}$, 4H), 5.73 (s, Ta(μ-*H*), 2H), 3.89 (br s, *H*B, 4H), 2.08 (s, *H*$_3$C$_{\text{Mes}}$, 12H, overlaps toluene-*d*$_8$ peak), 1.91 (s, *H*$_3$C$_{\text{Mes}}$, 12H), 1.81 (s, (C$_6$*H*$_6$, 6H), 1.78 (s, *H*$_3$C$_{\text{Mes}}$, 12H). ^{13}C NMR (151 MHz, toluene-*d*$_8$) δ = 203.1 (*C*$_{\text{Imid}}$), 137.8, 137.2, 136.5, 134.8, 129.2, 128.7, 128.6, 128.3 (H*C*$_{\text{Mes}}$), 128.2 (H*C*$_{\text{Mes}}$), 128.1, 125.4, 123.9 (H*C*$_{\text{Imid}}$), 120.3 (H*C*$_{\text{Imid}}$), 58.8 (*C*$_6$H$_6$), 21.1 (H$_3$*C*$_{\text{Mes}}$), 19.6 (H$_3$*C*$_{\text{Mes}}$), 18.2 (H$_3$*C*$_{\text{Mes}}$). ^{11}B NMR (193 MHz, toluene-*d*$_8$) δ = -14.54. FT-IR (KBr, Nujol, cm^{-1}) 2409 (m, $\nu_{\text{B-H}}$). Anal. calcd for $C_{54}H_{64}B_2N_8Ta_2$ (**4**): C, 53.66; H, 5.34; N, 9.27. Found: C, 53.60; H, 5.33; N, 9.31.

Method B. In the glovebox, compound **3·toluene** (50.0 mg, 0.0386 mmol) and 2 equivalents of KC_8 (10.4 mg, 0.0772 mmol) were combined in a 20 mL scintillation vial. Benzene (12 mL) was added to the solid mixture, resulting in a brown solution that immediately began to turn purple in color. The purple solution was stirred vigorously at ambient temperature for 12 h, resulting in a heterogeneous purple solution with fine solids (presumably graphite and KCl). The volatiles were removed via lyophilization to afford purple, amorphous solids. The solids were extracted with toluene (3 × 2 mL), and the combined extracts were filtered through Celite, concentrated to a final volume of ca. 0.25 mL, and stored at –40 °C overnight, yielding dark blue crystals of **4** (32.8 mg, 70% yield; molecular mass was calculated to include one equivalent of toluene solvent, as observed by ^{1}H NMR spectroscopy). The ^{1}H NMR spectrum of **4** synthesized using method B exactly matches that of **4** synthesized by method A.

{[H$_2$B($^{\text{Mes}}$Im)$_2$]Ta}$_2$(μ-H)$_2$(μ-η^4:η^4-C$_7$H$_8$) (5).

Method A. Compound **2·toluene** (250 mg, 0.348 mmol) was added to a 250 mL round-bottomed Schlenk flask and dissolved in toluene (10 mL). The solution was degassed, and the headspace was refilled with H_2. After 15 minutes, the solution changed color from bright yellow to orange. The flask was sealed, and the solution was stirred vigorously at ambient temperature for 24 h. Then, the H_2 was removed, the solution was degassed, and the headspace was refilled with N_2. The solution was stirred vigorously at ambient temperature for an additional 48 h. Over the course of the reaction, the solution progressed in color from orange to dark purple. The volatiles were removed under vacuum, and the dark purple, tacky solids were triturated with 5 mL hexane, resulting in a dark purple powder. The crude product was extracted with hexane (3 × 12 mL), and the combined extracts were filtered through Celite. The solvent was removed under vacuum, affording a dark purple powder. The dark purple powder was extracted with Et_2O (2 × 5 mL), and the combined extracts were filtered through Celite, concentrated to a final volume of ca. 2 mL, and stored at –40 °C overnight, yielding dark purple crystals of **5** (163 mg, 77% yield). X-ray quality crystals of **5·hexane** were grown by vapor diffusion of hexane into a saturated toluene solution of **5** at room temperature. Mp 174 °C (decomp). ^{1}H NMR (500 MHz, C_6D_6) δ = 6.90 (d, *J* = 1.3 Hz, *H*C$_{\text{Imid}}$, 4H), 6.72 (s, *H*C$_{\text{Mes}}$, 4H), 6.66 (s, *H*C$_{\text{Mes}}$, 4H), 6.13 (d, *J* = 1.0 Hz, *H*C$_{\text{Imid}}$, 4H), 5.75 (s, Ta(μ-*H*), 2H), 3.55 (br s, *H*B, 4H), 2.33 (br s, *H*C$_{\text{tol}}$, 1H), 2.05 (br s, *H*C$_{\text{tol}}$, 2H), 2.01 (s, *H*$_3$C$_{\text{Mes}}$, 24H), 1.88 (br s, *H*C$_{\text{tol}}$, 2H), 1.84 (s, *H*$_3$C$_{\text{Mes}}$, 12H), 0.96 (br s, *H*$_3$C$_{\text{tol}}$, 3H). ^{13}C NMR (151 MHz, C_6D_6) δ = 203.0 (*C*$_{\text{Imid}}$), 138.0, 137.5, 136.5, 135.2, 128.9, 128.8 (H*C*$_{\text{Mes}}$), 128.4 (H*C*$_{\text{Mes}}$), 124.1 (H*C*$_{\text{Imid}}$), 120.7 (H*C*$_{\text{Imid}}$), 64.1 (H*C*$_{\text{tol}}$), 57.9 (H*C*$_{\text{tol}}$), 23.1 (H$_3$*C*$_{\text{tol}}$), 21.0 (H$_3$*C*$_{\text{Mes}}$), 18.6 (H$_3$*C*$_{\text{Mes}}$). ^{11}B NMR (193 MHz, C_6D_6) δ = -14.41. FT-IR (KBr, Nujol, cm^{-1}) 2421 (m, $\nu_{\text{B-H}}$). Anal. Calcd for $C_{55}H_{66}B_2N_8Ta_2$ (**5**): C, 54.03; H, 5.44; N, 9.16. Found: C, 53.94; H, 5.59; N, 9.06.

Method B. In the glovebox, compound **3·toluene** (32.0 mg, 0.0247 mmol) and 2 equivalents of KC_8 (6.68 mg, 0.0494 mmol) were combined in a 20 mL scintillation vial. Toluene (8 mL) was added to the solid mixture, resulting in a brown solution that immediately began to turn purple in color. The purple solution was stirred vigorously at ambient temperature for 12 h, resulting in a heterogeneous purple solution with fine solids (presumably graphite and KCl). The volatiles were removed under vacuum, affording purple, amorphous solids. The solids were extracted with ether (3 × 2 mL), and the combined extracts were filtered through Celite, concentrated to a final volume of ca. 0.25 mL, and stored at 22 ^{o}C overnight, yielding dark purple crystals of **5** (33.7 mg, 71% yield). The ^{1}H NMR spectrum of **5** synthesized using method B exactly matches that of **5** synthesized by method A.

$\{[H_2B(^{Mes}Im)_2]Ta\}\{(^{Mes}Im)H_2B[Im(2,4\text{-}CH_3\text{-}6\text{-}\mathit{C}H_2\text{-}C_6H_2)]Ta\}_2(\mu\text{-}H)_4$ (6). Compound **2·toluene** (250 mg, 0.348 mmol) was added to a 250 mL round-bottomed Schlenk flask and dissolved in hexane (25 mL). The solution was degassed, and the headspace was refilled with H_2. After 15 minutes, the solution changed color from bright yellow to orange. The flask was sealed, and the solution was stirred vigorously at ambient temperature for 3 days; over the course of the reaction, the solution progressed in color from orange to a dark purple suspension. The dark purple solids were collected on a fine-porosity fritted glass filter, washed with hexane (2 × 10 mL), and dried under vacuum. Then, the crude product was extracted with toluene (3 × 10 mL), and the combined extracts were filtered through Celite, concentrated to a final volume of ca. 3 mL, and stored at –40 ^{o}C overnight, yielding dark purple crystals of **6** (116 mg, 56% yield; the molecular mass was calculated to include one equivalent of toluene solvent, as observed by ^{1}H NMR spectroscopy). X-ray quality crystals of **6·hexane** were grown by vapor diffusion of hexane into a saturated toluene solution of **6** at room temperature. Mp 213 °C (decomp). ^{1}H NMR (500 MHz, C_6D_6) δ = 10.48 (br s, Ta(μ-*H*), 2H), 9.03 (br s, Ta(μ-*H*), 1H), 8.47 (br s, Ta(μ-*H*), 1H), 7.65 (d, *J* = 1.4 Hz, HC_{Imid}, 1H), 7.53 (s, HC_{Ar}, 1H), 7.40 (d, *J* = 1.3 Hz, HC_{Imid}, 1H), 7.30 (s, HC_{Ar}, 1H), 7.09 (s, HC_{Ar}, 1H, overlaps toluene solvent peak), 6.94 (d, *J* = 1.3 Hz, HC_{Imid}, 1H), 6.93 (s, HC_{Ar}, 1H), 6.85 (s, HC_{Ar}, 1H), 6.80 (d, *J* = 1.3 Hz, HC_{Imid}, 1H), 6.59 (s, HC_{Ar}, 1H), 6.57 (s, HC_{Ar}, 1H), 6.56 (s, HC_{Ar}, 1H), 6.52 (d, *J* = 1.4 Hz, HC_{Imid}, 1H), 6.50 (d, *J* = 1.4 Hz, HC_{Imid}, 1H), 6.49 (d, *J* = 1.4 Hz, HC_{Imid}, 1H), 6.48 (s, HC_{Ar}, 1H), 6.43 (s, HC_{Ar}, 2H), 6.34 (d, *J* = 1.3 Hz, HC_{Imid}, 1H), 6.32 (s, HC_{Ar}, 1H), 6.30 (d, *J* = 1.4 Hz, HC_{Imid}, 1H), 6.03 (d, *J* = 1.4 Hz, HC_{Imid}, 1H), 5.97 (d, *J* = 1.4 Hz, HC_{Imid}, 1H), 5.58 (d, *J* = 1.4 Hz, HC_{Imid}, 1H), 4.60 (br s, *H*B, 6H), 3.25 (s, H_3C_{Mes}, 3H), 2.79 (s, H_3C_{Mes}, 3H), 2.53 (s, H_3C_{Mes}, 3H), 2.47 (s, H_3C_{Mes}, 3H), 2.41 (d, *J* = 9.8 Hz, H_2C_{Ar}, 2H), 2.20 (s, H_3C_{Mes}, 6H), 2.14 (s, H_3C_{Mes}, 3H), 2.07 (s, H_3C_{Mes}, 3H), 2.05 (s, H_3C_{Mes}, 3H), 1.70 (s, H_3C_{Mes}, 3H), 1.69 (s, H_3C_{Mes}, 3H), 1.64 (s, H_3C_{Mes}, 3H), 1.42 (s, H_3C_{Mes}, 3H), 1.41 (s, H_3C_{Mes}, 3H), 1.40 (s, H_3C_{Mes}, 3H), 0.65 (d, *J* = 9.8 Hz, H_2C_{Ar}, 2H). ^{13}C NMR (151 MHz, C_6D_6) δ = 151.1, 138.6, 138.3, 138.1, 137.63, 137.59, 137.1, 136.84, 136.80, 136.7, 136.5, 136.39, 136.35, 136.33, 136.2, 135.3, 135.2, 135.1, 134.3, 133.44, 133.43, 132.5, 129.9, 129.8, 129.63, 129.59, 128.9, 128.62, 127.71, 126.69, 125.4, 124.4, 123.0, 122.6, 122.2, 122.0, 121.9, 121.8, 121.0, 120.5, 120.4, 119.3, 64.3 (H_2C_{Ar}), 23.4 (H_3C_{Mes}), 23.3 (H_3C_{Mes}), 22.7 (H_3C_{Mes}), 21.9 (H_3C_{Mes}), 21.7 (H_3C_{Mes}), 21.6 (H_3C_{Mes}), 21.5 (H_3C_{Mes}), 21.3 (H_3C_{Mes}), 20.9 (H_3C_{Mes}), 20.8 (H_3C_{Mes}), 20.5 (H_3C_{Mes}), 20.2 (H_3C_{Mes}), 19.1 (H_3C_{Mes}), 18.6 (H_3C_{Mes}), 18.1 (H_3C_{Mes}), 17.8 (H_3C_{Mes}). ^{11}B NMR (193 MHz, C_6D_6) δ = -14.42, -16.87. FT-IR (KBr, Nujol, cm^{-1}) 2454 (m, $\nu_{B\text{-}H}$), 2353 (m, $\nu_{B\text{-}H}$), 2258 (w, $\nu_{B\text{-}H}$), 2015 (m, $\nu_{B\text{-}H}$). Anal. calcd for $C_{72}H_{86}B_3N_{12}Ta_3$ (**6**): C, 51.03; H, 5.11; N, 9.92. Found: C, 51.28; H, 5.26; N, 9.81.

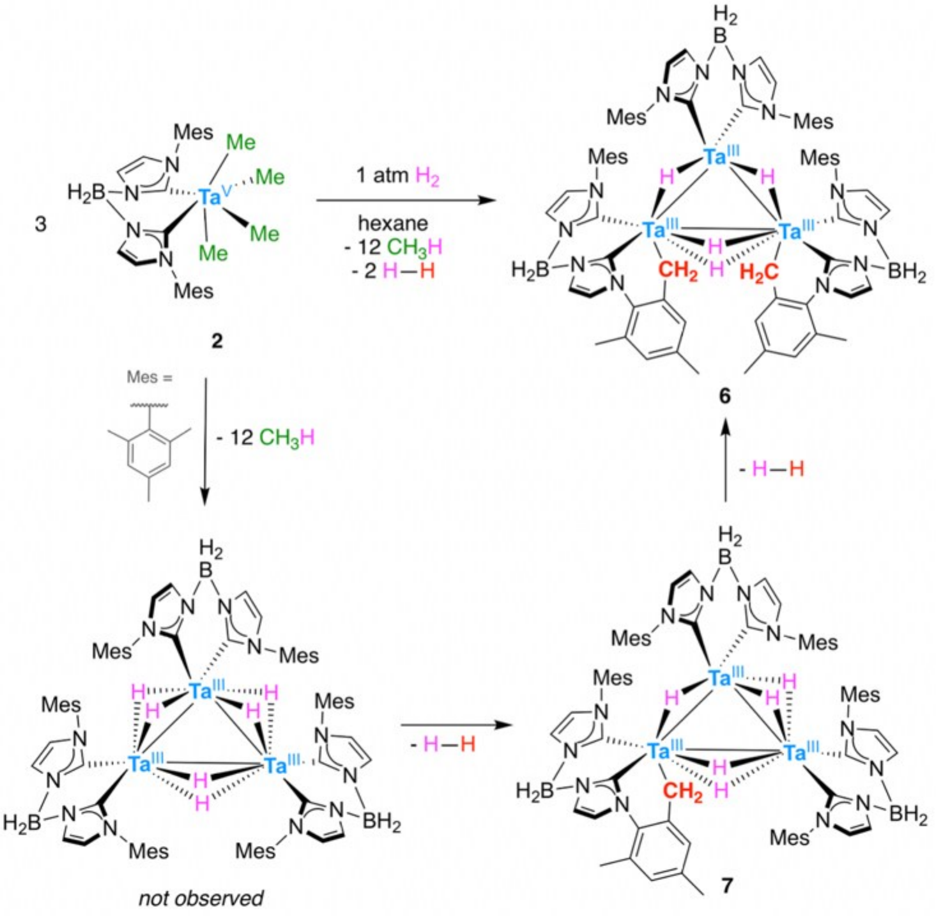

Scheme S2. Synthesis of complex **6** via hydrogenolysis of **2**, proceeding through intermediate **7**.

{[H$_2$B(^{Mes}Im)$_2$]Ta}$_2${(^{Mes}Im)H$_2$B[Im(2,4-CH$_3$-6-*C*H$_2$-C$_6$H$_2$)]Ta}(μ-H)$_5$ (7). We were able to access a crystalline mixture of compounds **6** and **7** when the normal hydrogenolysis reaction time of three days was truncated; crystallization yielded a mixture of products. Compound **2·toluene** (25 mg, 0.0348 mmol) was added to a 100 mL round-bottomed Schlenk flask and dissolved in hexane (10 mL). The solution was degassed, and the headspace was refilled with H_2. After 15 minutes, the solution changed color from bright yellow to orange. The flask was sealed, and the solution was stirred vigorously at ambient temperature for 12 h; over the course of the reaction, the solution progressed in color from orange to a dark purple suspension. The dark purple solids were collected on a fine fritted glass filter, washed with hexane (2 × 10 mL), and dried under vacuum. Then, the crude product was extracted with toluene (3 × 2 mL), and the combined extracts were filtered through Celite, concentrated to a final volume of ca. 0.5 mL, and stored at $-40\ ^{o}C$ overnight, yielding dark purple crystals of **6** and **7**. Pure samples of **7** could not be isolated, as **7** is an intermediate that converts to **6** in solution; as such, the yield, melting point and elemental analysis data, and NMR and FT-IR spectroscopic characterization could not be obtained. X-ray quality crystals of **7** were grown by vapor diffusion of hexane into a saturated toluene solution of **6** and **7** at room temperature over a period of two hours.

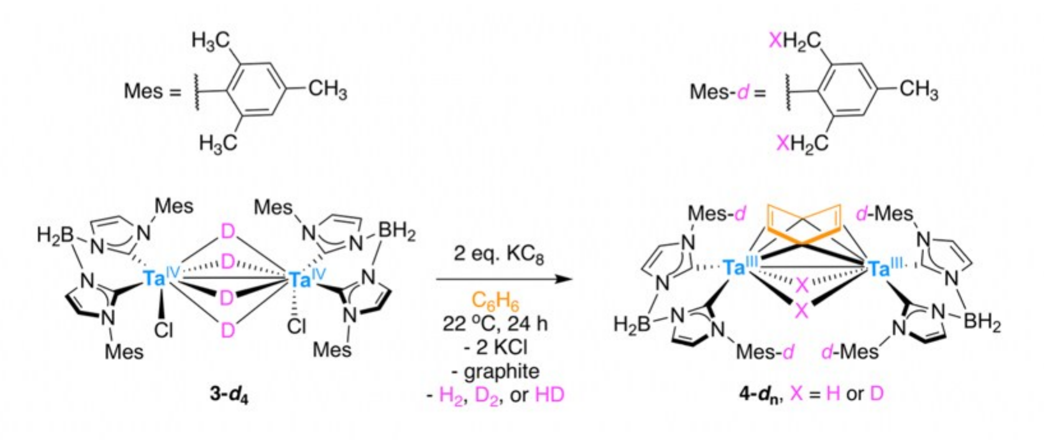

Scheme S3. Synthesis of complex **4-*d*$_n$**.

Reaction of 3-*d*$_4$ with KC_8 in C_6H_6. In the glovebox, compound **3-*d*$_4$·toluene** (31.5 mg, 0.0242 mmol) and 2 equivalents of KC_8 (6.53 mg, 0.04833 mmol) were combined in a 20 mL scintillation vial. Benzene (5 mL) was added to the solid mixture, resulting in a brown solution that immediately began to turn purple in color. The purple solution was stirred vigorously at ambient temperature for 24 h, resulting in a heterogeneous purple solution with fine solids (presumably graphite and KCl). The volatiles were removed via lyophilization to afford purple, amorphous solids. The solids were extracted with toluene (2 × 4 mL), and the combined extracts were filtered through Celite, concentrated to a final volume of ca. 0.25 mL, and stored at –40 °C overnight, yielding dark blue crystals of $\{[H_2B(^{Mes\text{-}H/D}Im)_2]Ta\}_2(\mu\text{-}H/D)_2(\mu\text{-}\eta^4{:}\eta^4\text{-}C_6H_6)$ (**4-*d*$_n$**; 18.9 mg, 60% yield; molecular mass was calculated to include one equivalent of toluene solvent, as observed by ^{1}H NMR spectroscopy). ^{1}H NMR (600 MHz, C_6D_6) δ = 6.90 (s, HC_{Imid}, 4H), 6.74 (s, HC_{Mes}, 4H), 6.63 (s, HC_{Mes}, 4H), 6.13 (s, HC_{Imid}, 4H), 5.88 (s, Ta(μ-*H*)$_n$, 1H), 3.14 (br s, *H*B, 4H), 2.03 (s, H_3C_{Mes}, 12 H), 2.02 (s, C_6H_6, 6H), 1.93 (s, H_3C_{Mes}, 9H), 1.92 (s, $D_nH_{3\text{-}n}C_{Mes\text{-}H/D}$, 2H), 1.85 (s, H_3C_{Mes}, 9H), 1.84 (s, $D_nH_{3\text{-}n}C_{Mes\text{-}H/D}$, 2H). ^{2}H NMR (92 MHz, C_6H_6) δ = 5.85 (br s, Ta(μ-*D*)$_n$, 1D), 1.86 (br s, $D_nH_{3\text{-}n}C_{Mes\text{-}H/D}$, 6D).

B. NMR and IR Spectroscopic Data

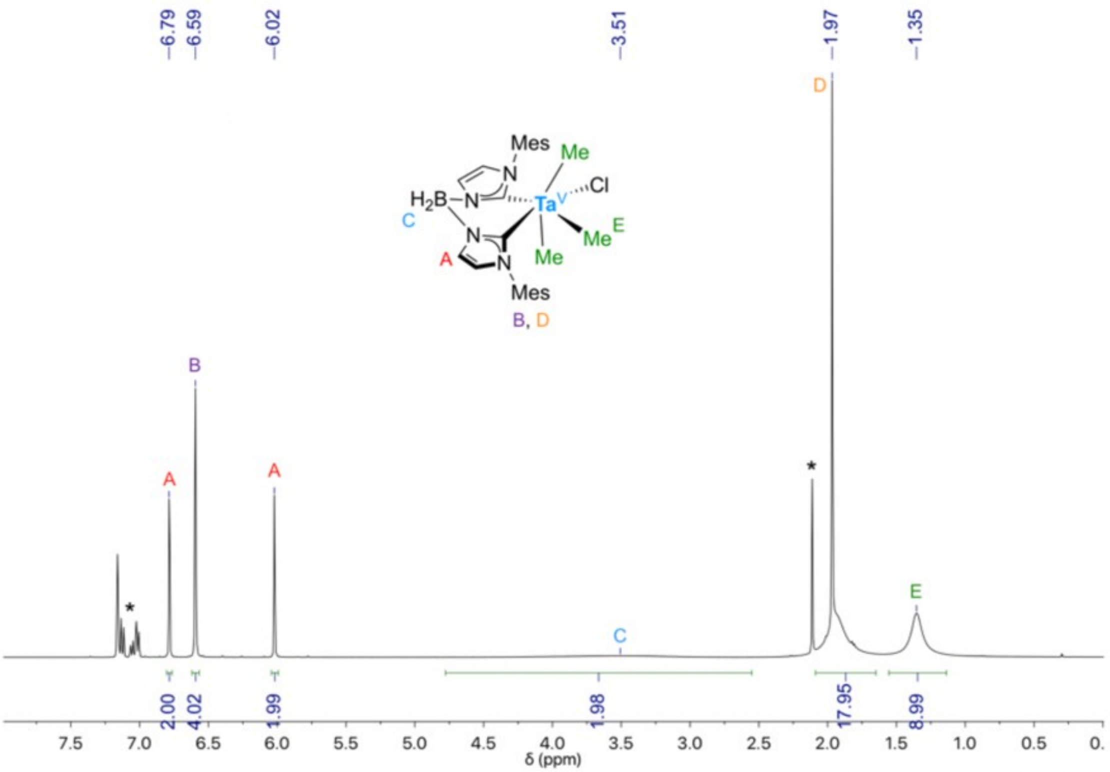

Figure S1. ^{1}H NMR spectrum of **1** in C_6D_6 (295 K, 400 MHz). *Toluene.

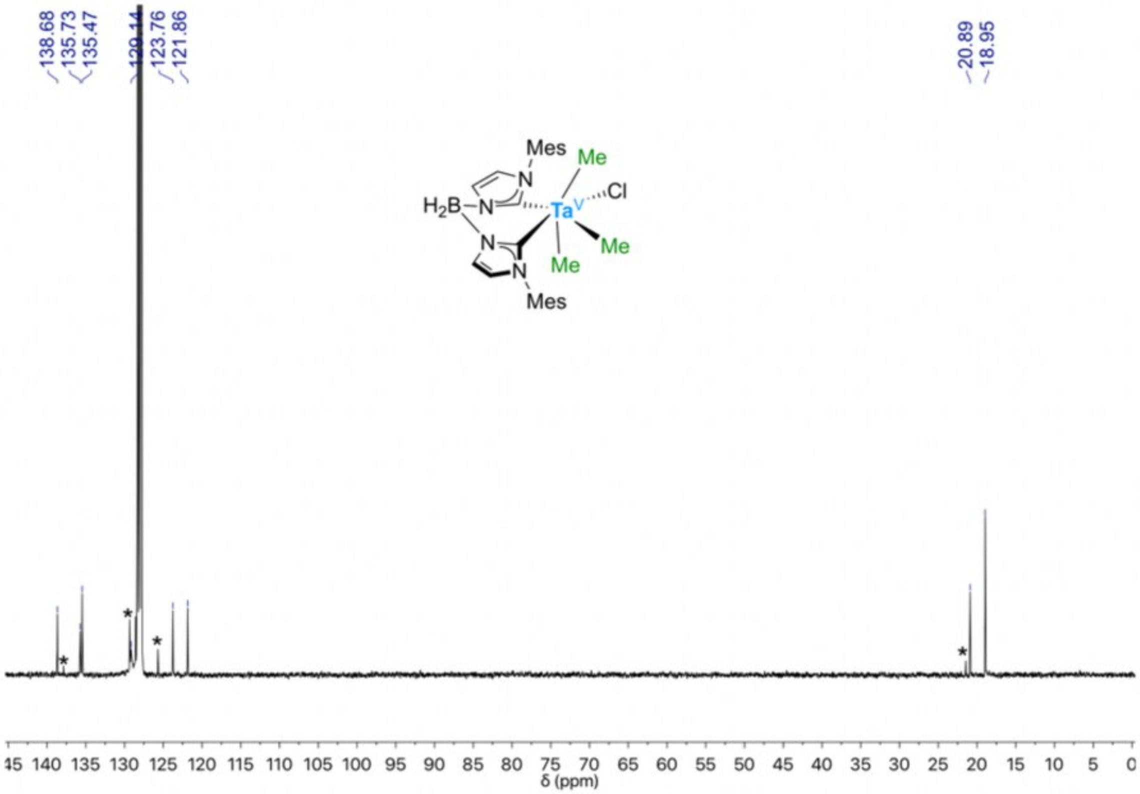

Figure S2. ^{13}C NMR spectrum of **1** in C_6D_6 (295 K, 101 MHz). *Toluene

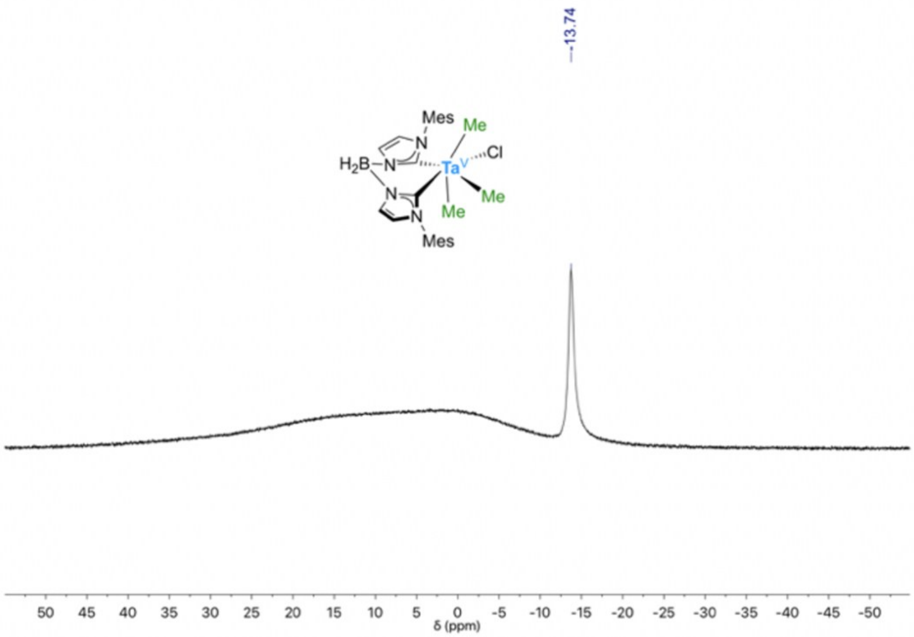

Figure S3. ^{11}B NMR spectrum of **1** in C_6D_6 (295 K, 193 MHz). The broad resonance centered about δ 5 originates from the borosilicate glass NMR tube.

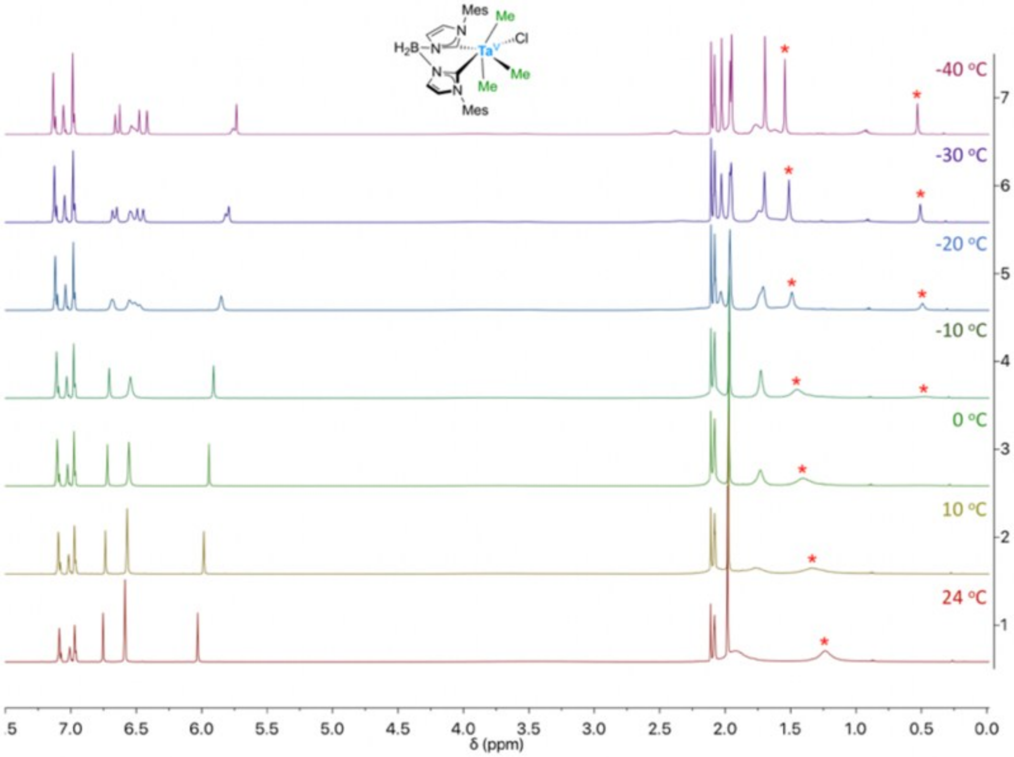

Figure S4. Variable temperature ^{1}H NMR spectra of **1** in toluene-d_8 (233-297 K, 600 MHz). *The three Ta–Me groups resolve into sharp resonances as the temperature is lowered; at –40 °C, the Ta–Me resonances at δ 1.54 and 0.53 integrate to six and three protons, respectively.

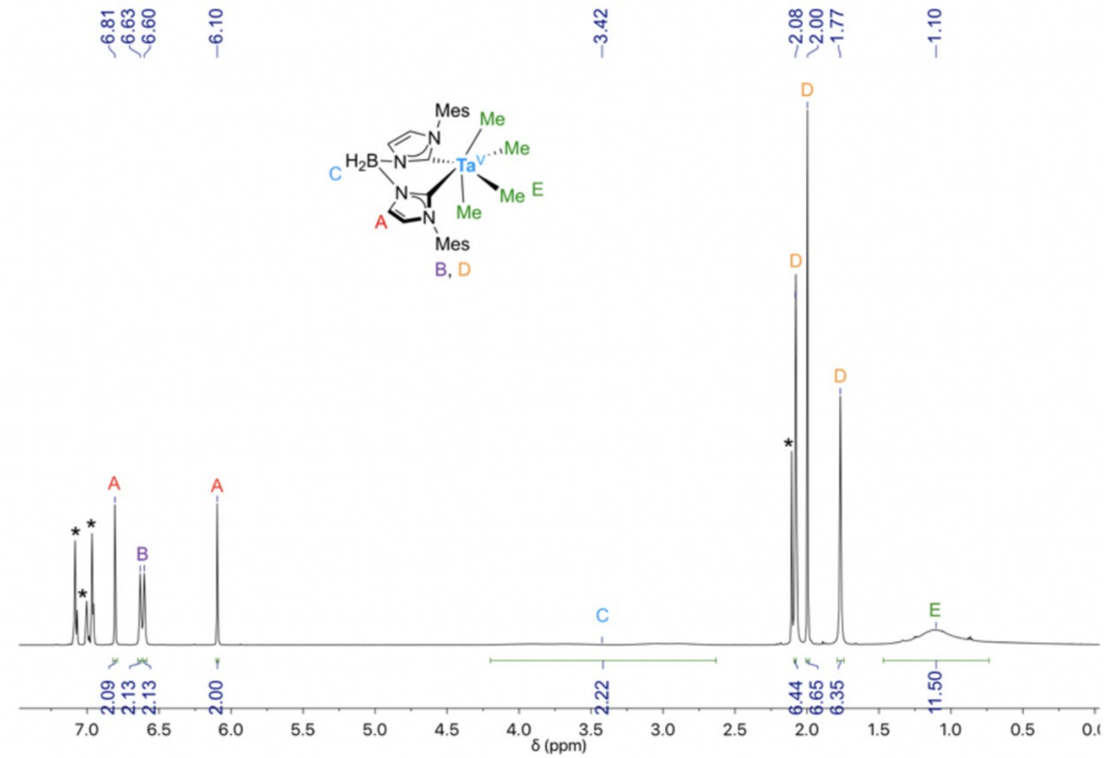

Figure S5. ^{1}H NMR spectrum of **2** in toluene-d_8 (295 K, 600 MHz). *Toluene.

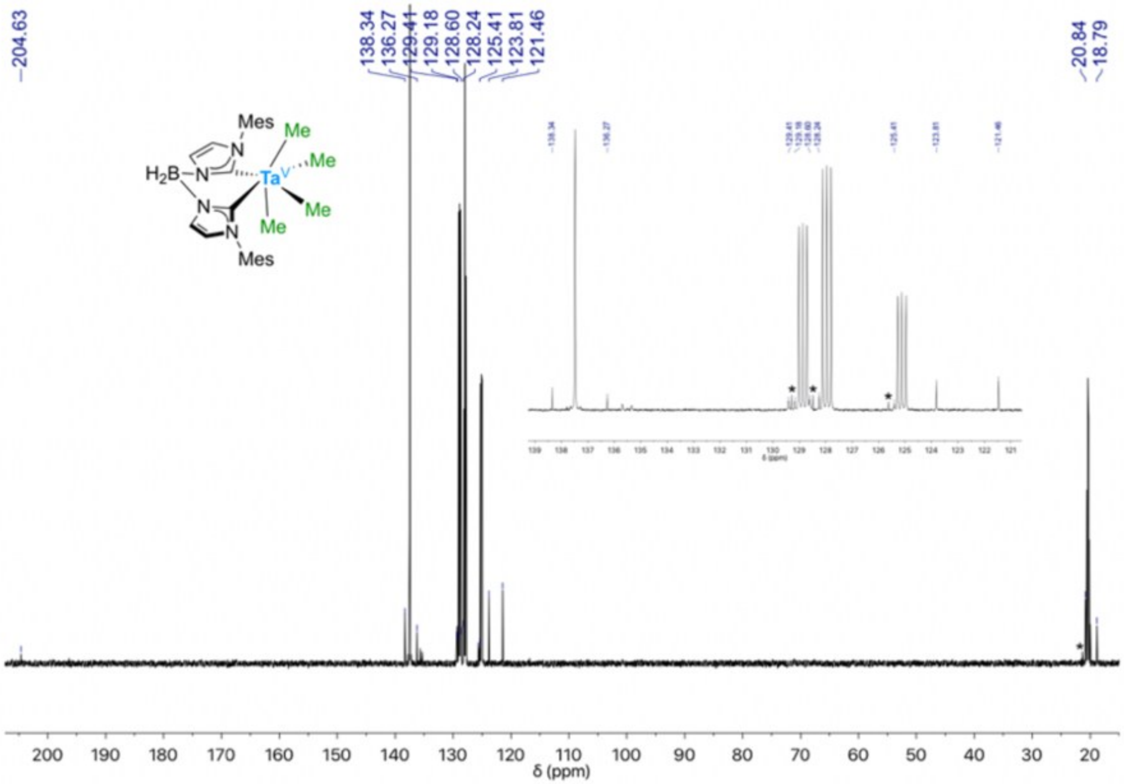

Figure S6. ^{13}C NMR spectrum of **2** in toluene-d_8 (295 K, 151 MHz). *Toluene.

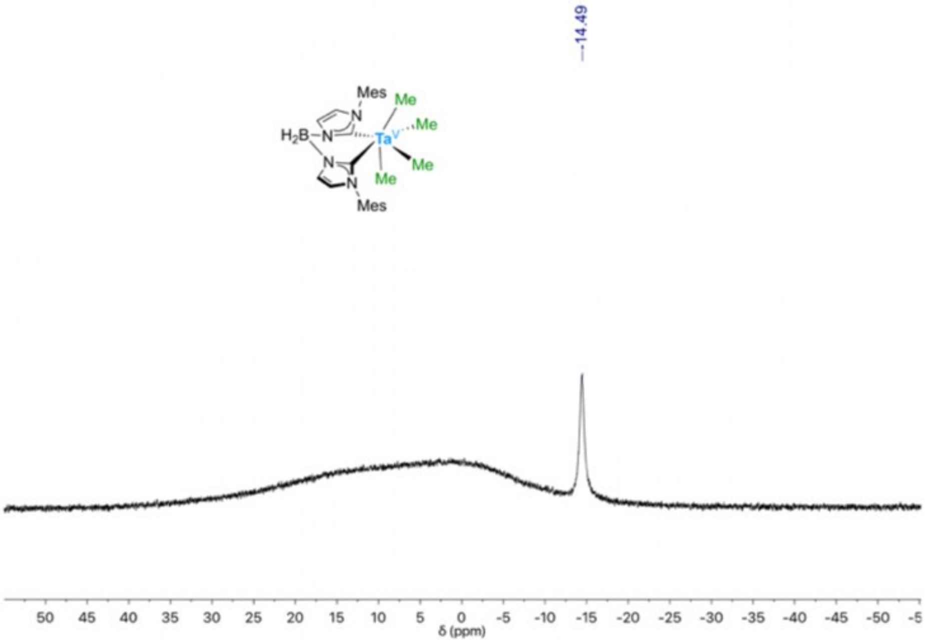

Figure S7. ^{11}B NMR spectrum of **2** in toluene-d_8 (295 K, 193 MHz). The broad resonance centered about δ 5 originates from the borosilicate glass NMR tube.

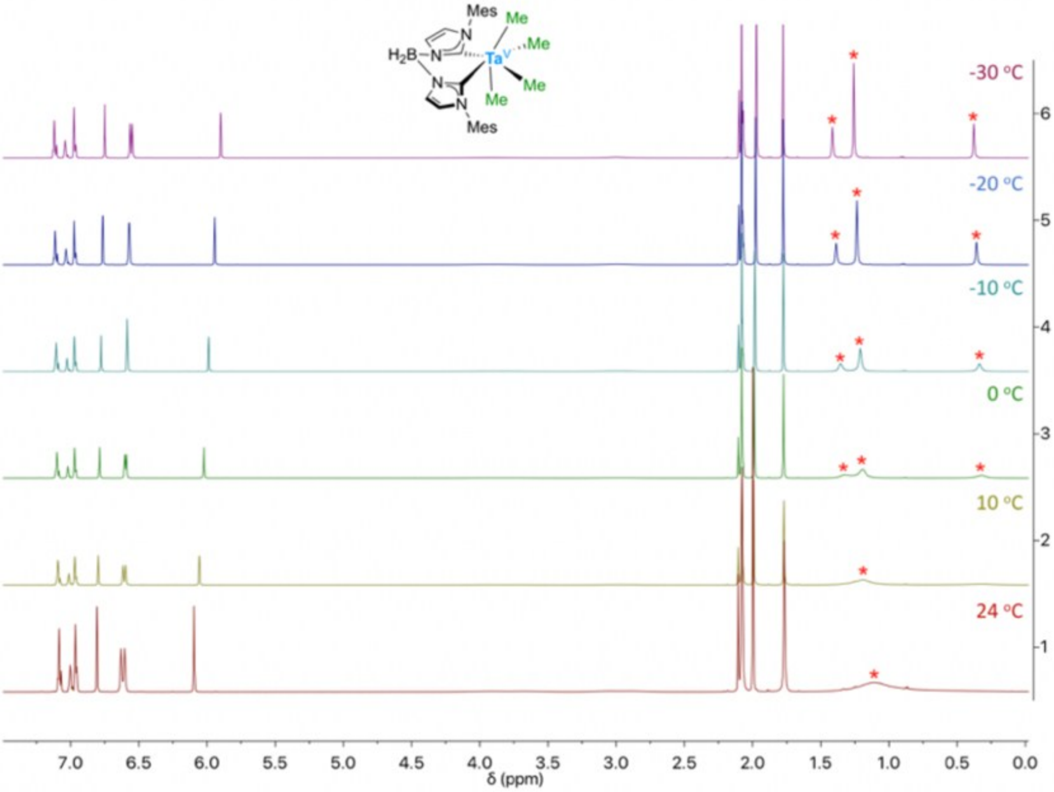

Figure S8. Variable temperature ^{1}H NMR spectra of **2** in toluene-d_8 (243-297 K, 600 MHz). *The three Ta–Me groups resolve into sharp resonances as the temperature is lowered; at –30 °C, the Ta–Me resonances at δ 1.41, 1.26, and 0.38 integrate to three, six, and three protons, respectively.

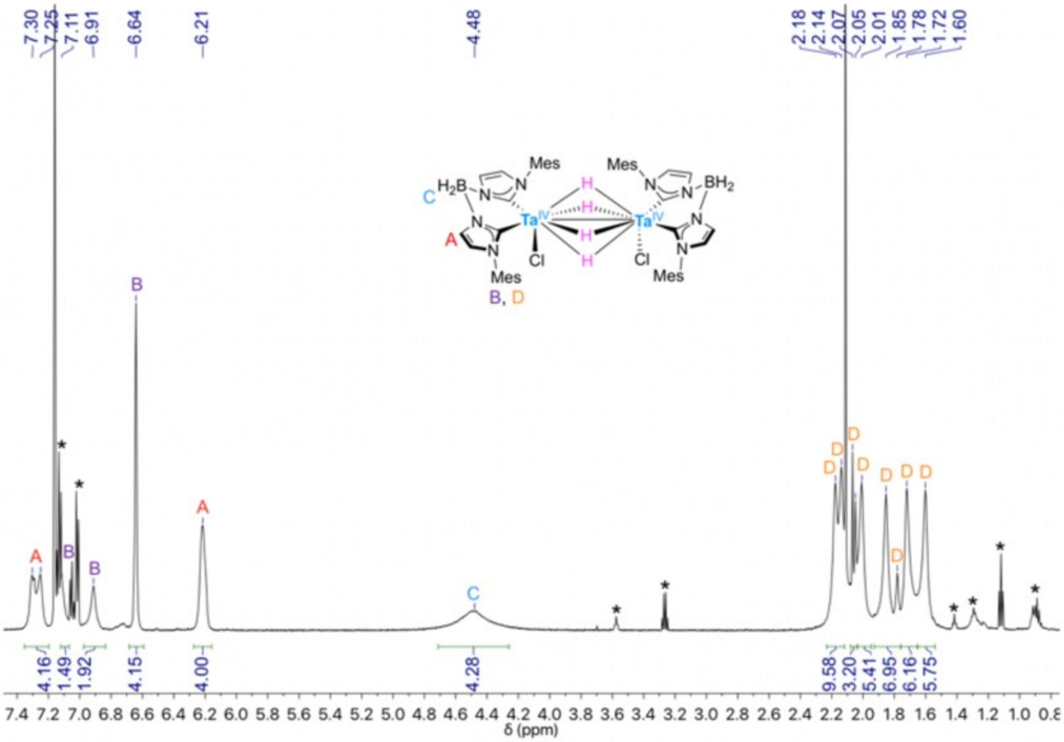

Figure S9. ^{1}H NMR spectrum of **3** in C_6D_6 (295 K, 600 MHz). *Toluene, hexane, THF, and Et_2O.

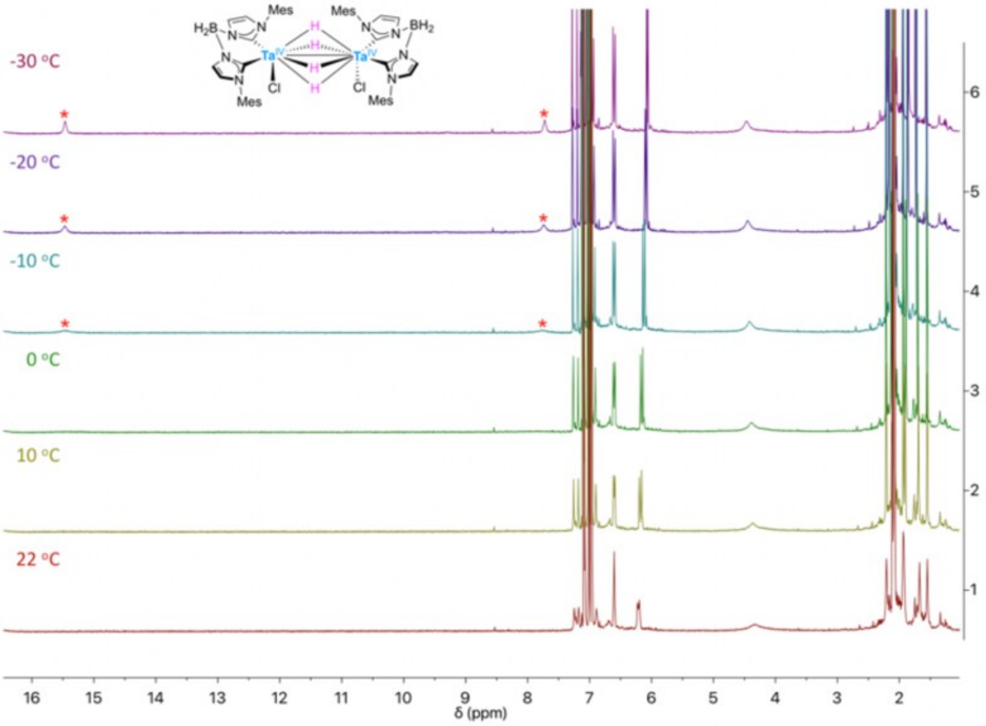

Figure S10. Variable temperature ^{1}H NMR spectra of **3** in toluene-d_8 (243-295 K, 600 MHz). *The bridging hydrides begin to appear at –10 °C and resolve into to two sharp resonances as the temperature is lowered; at –30 °C, the bridging hydride resonances at δ 15.45 and 7.70 integrate to two protons each.

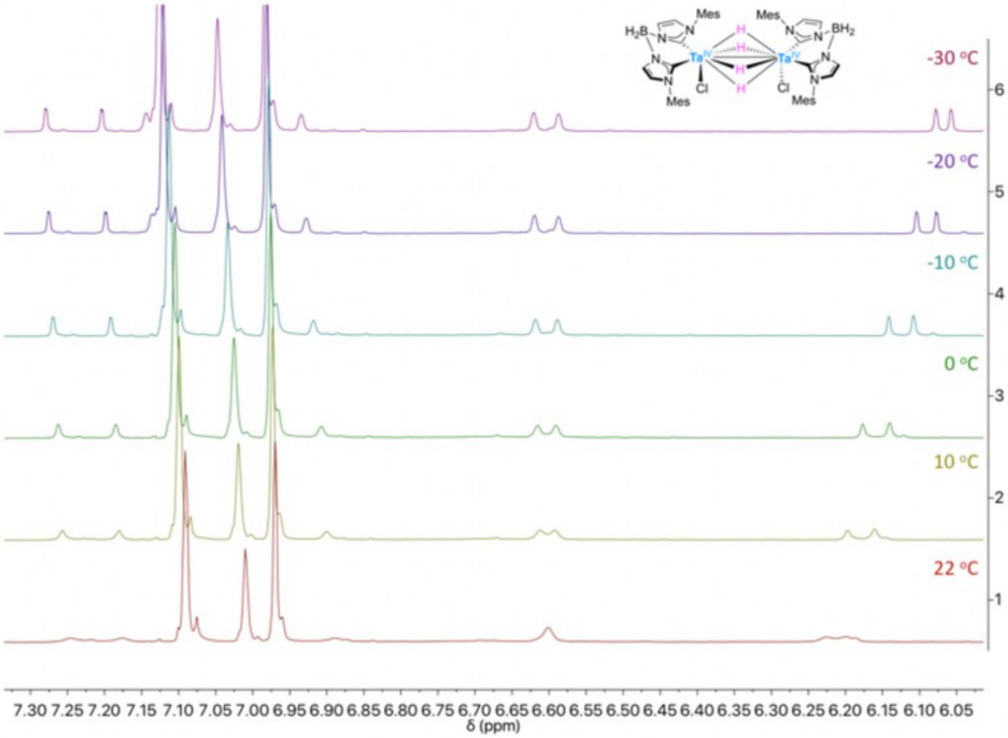

Figure S11. Variable temperature ^{1}H NMR spectra of **3** in toluene-d_8 (243-295 K, 600 MHz). As the temperature is lowered, the resonances for the imidazole protons and the arene protons of the mesityl groups begin to resolve and sharpen.

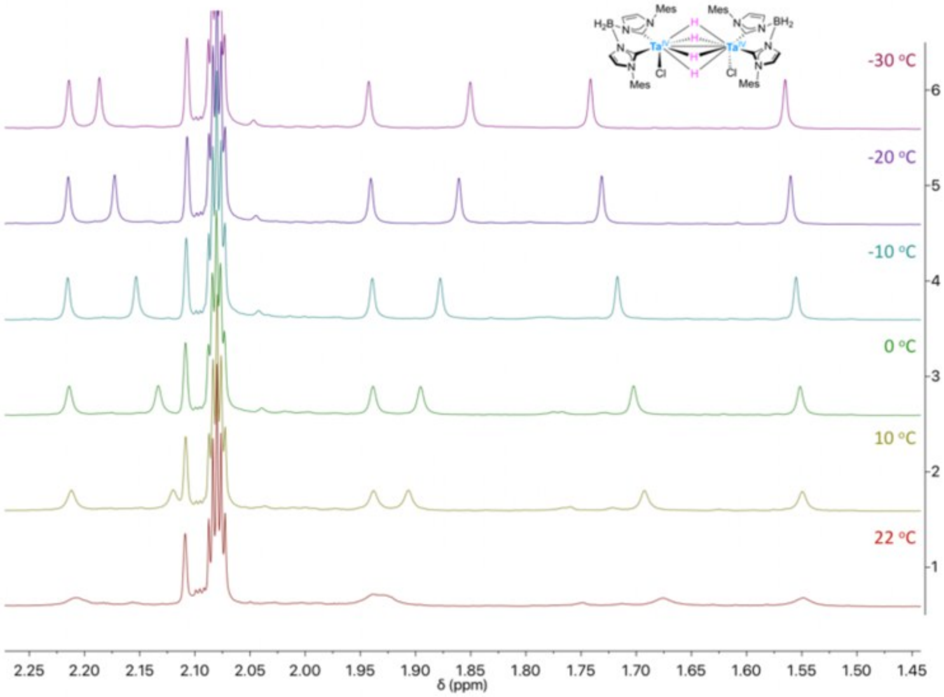

Figure S12. Variable temperature ^{1}H NMR spectra of **3** in toluene-d_8 (243-295 K, 600 MHz). As the temperature is lowered, the resonances for the methyl protons of the mesityl groups begin to sharpen into six resonances, integrating to three protons each.

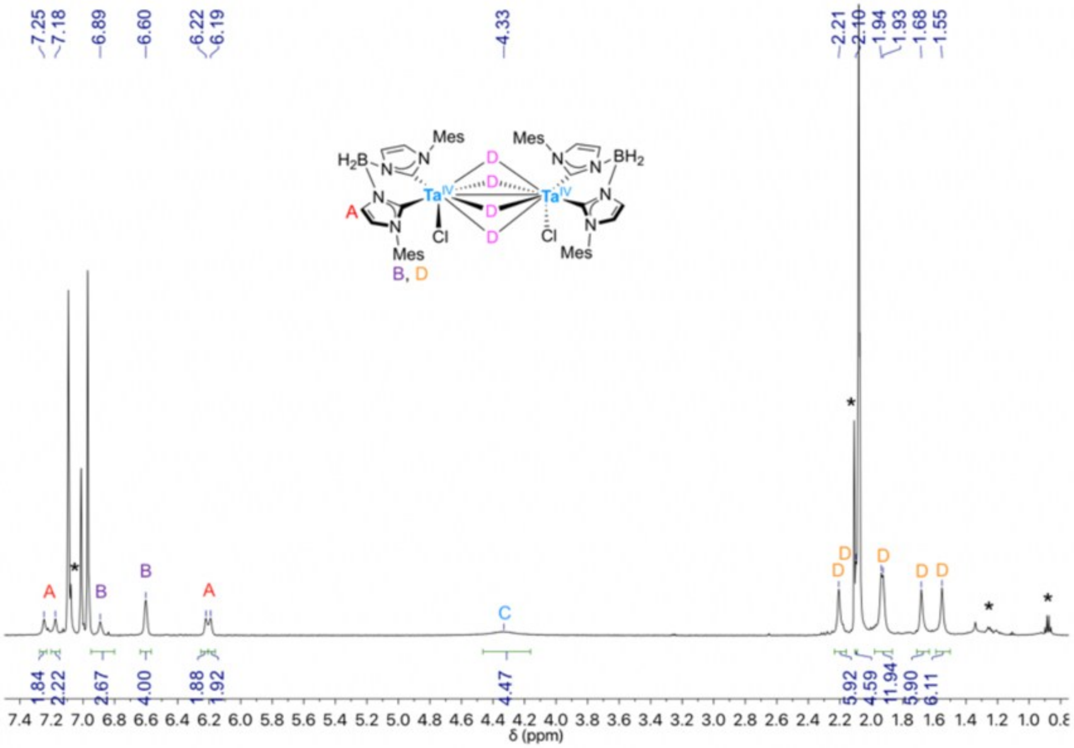

Figure S13. ^{1}H NMR spectrum of **3-*d*$_4$** in toluene-*d*$_8$ (295 K, 600 MHz). *Toluene and hexane.

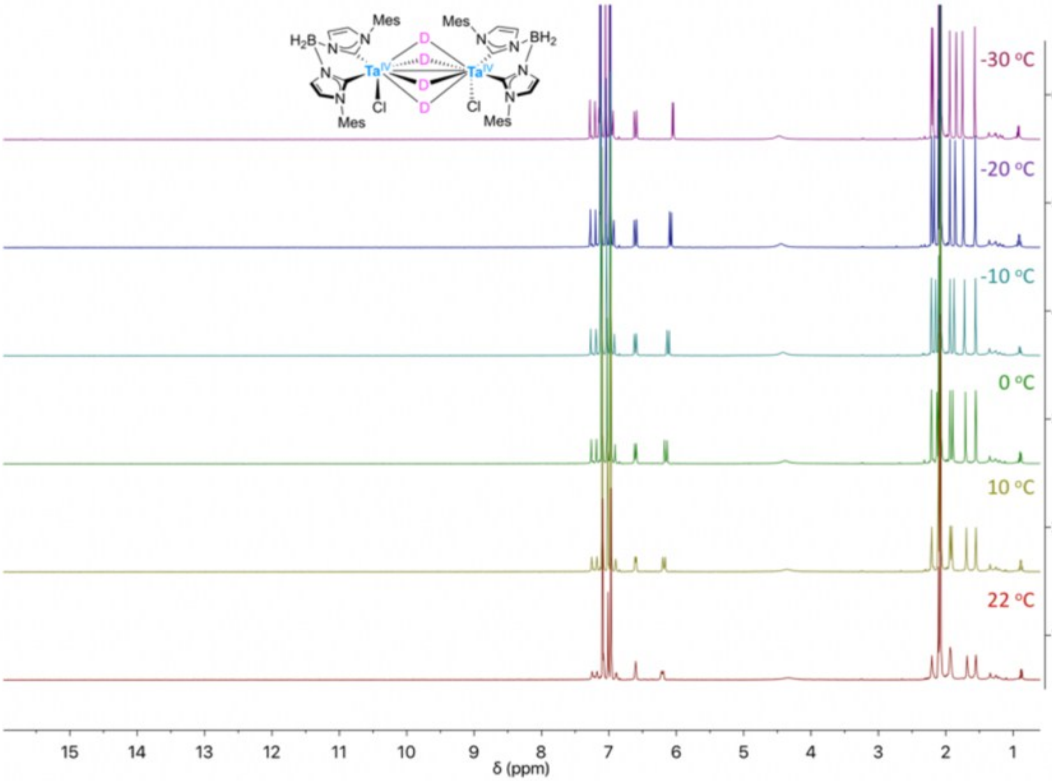

Figure S14. Variable temperature ^{1}H NMR spectra of **3-*d*$_4$** in toluene-*d*$_8$ (243-295 K, 600 MHz). Note the absence of resonances at δ 15.45 and 7.70 for the bridging deuterides at –30 °C.

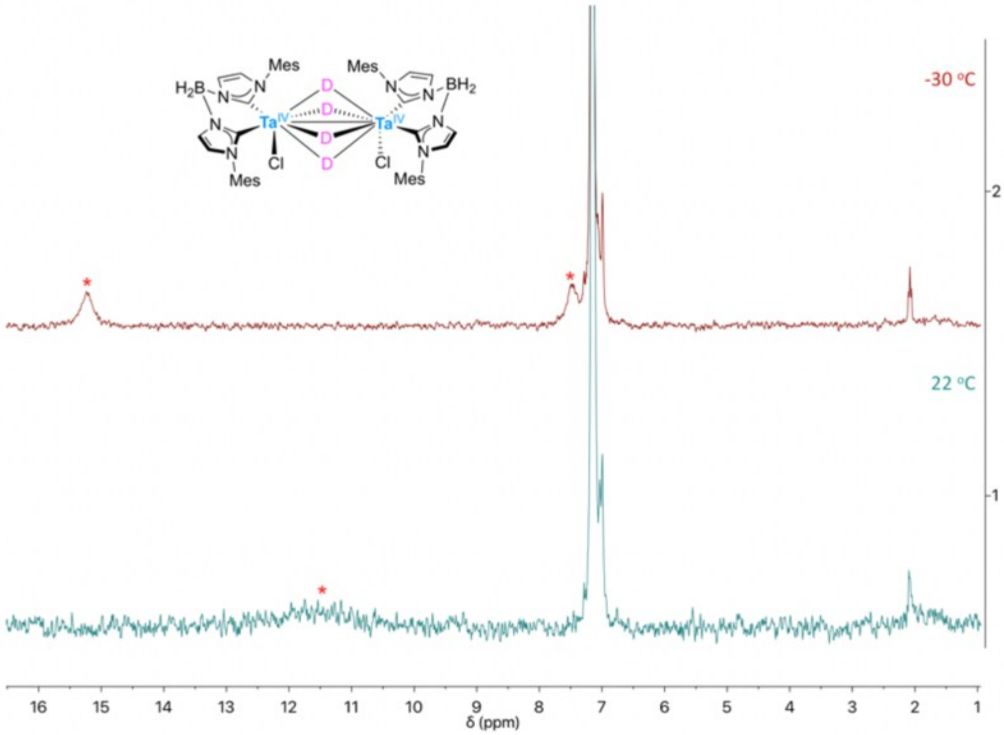

Figure S15. Variable temperature ^{2}H NMR spectra of **3-*d*$_4$** in toluene, referenced to a C_6D_6 internal standard (295 and 243 K, 92.1 MHz). *The bridging deuterides resolve into to two sharp resonances at –30 °C, appearing at δ 15.20 and 7.45.

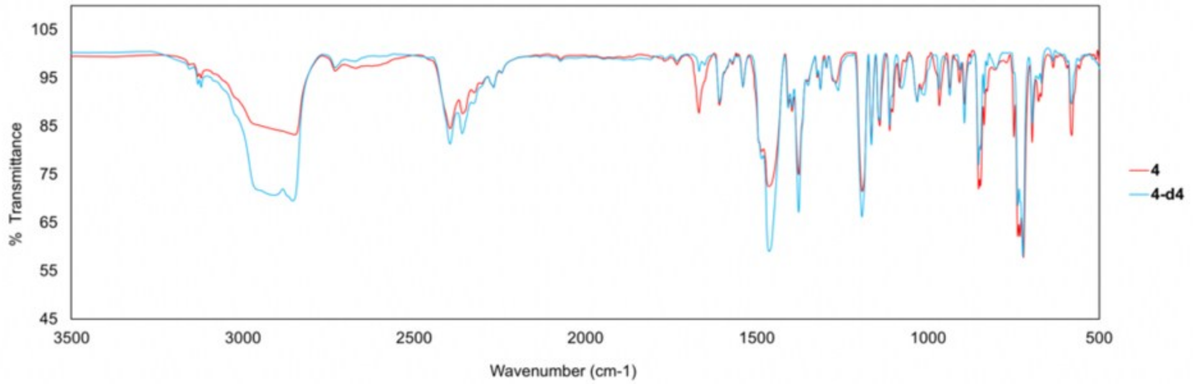

Figure S16. FT-IR spectra of **3** and **3-*d*$_4$**.

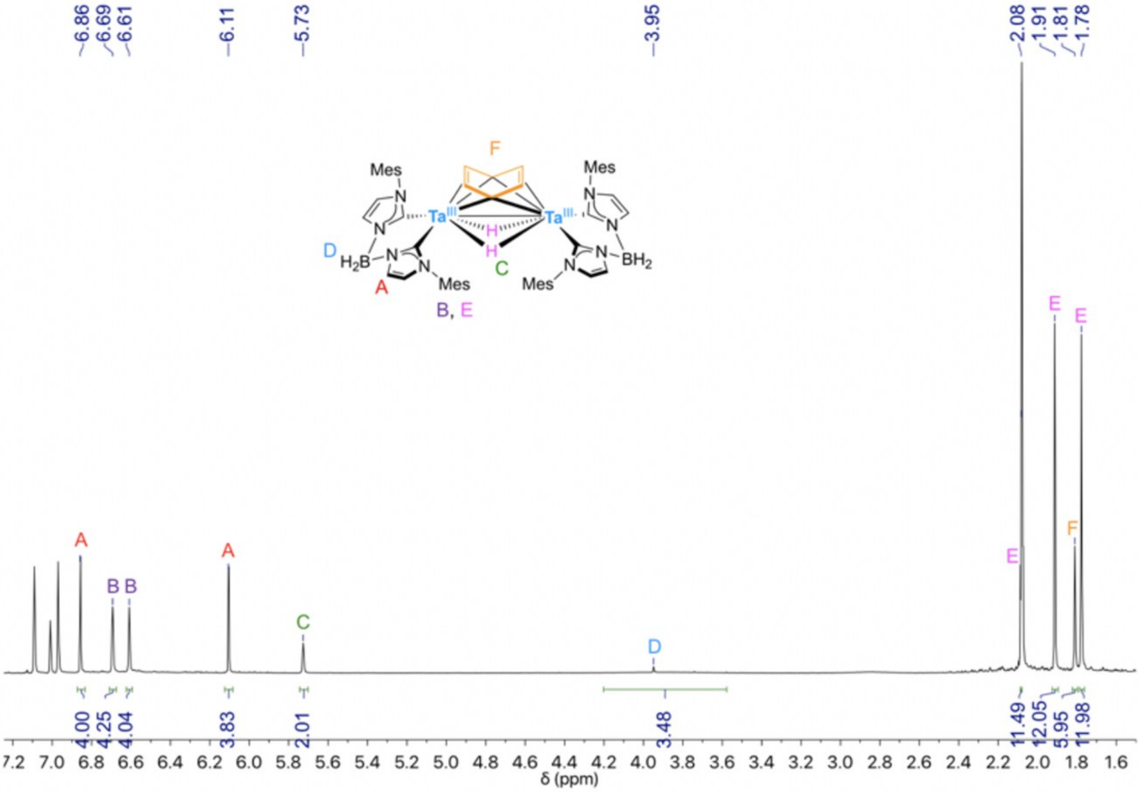

Figure S17. ^{1}H NMR spectrum of **4** in toluene-d_8 (295 K, 600 MHz).

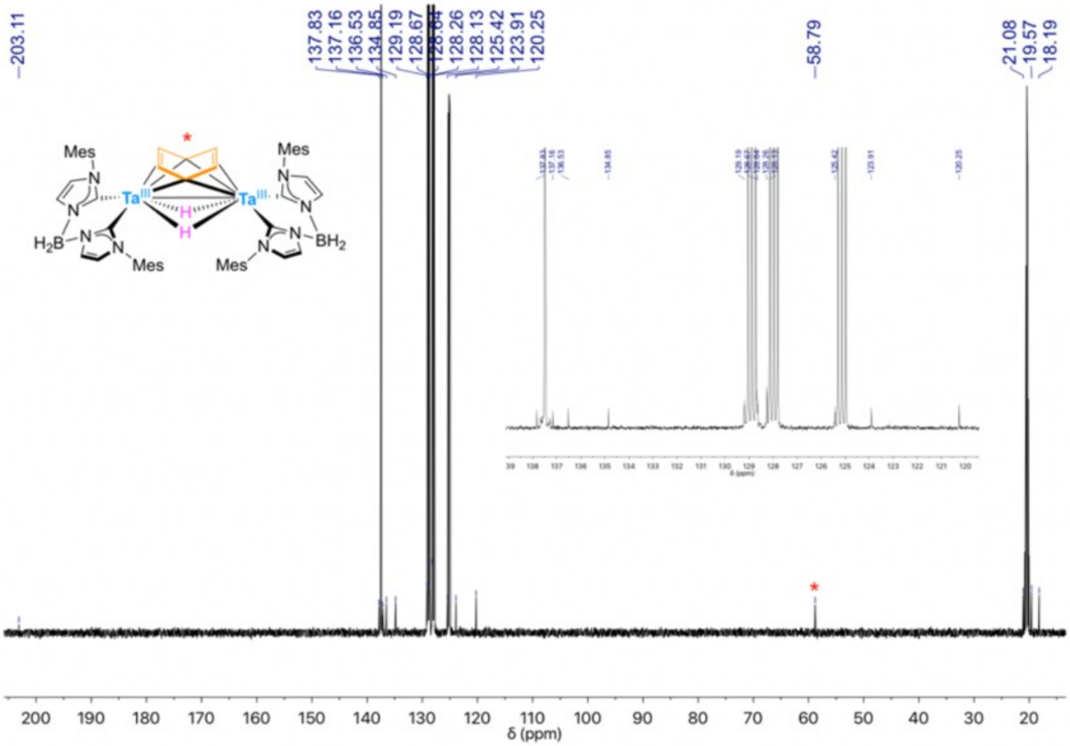

Figure S18. ^{13}C NMR spectrum of **4** in toluene-d_8 (295 K, 151 MHz). *The direduced benzene ligand appears at δ 58.8.

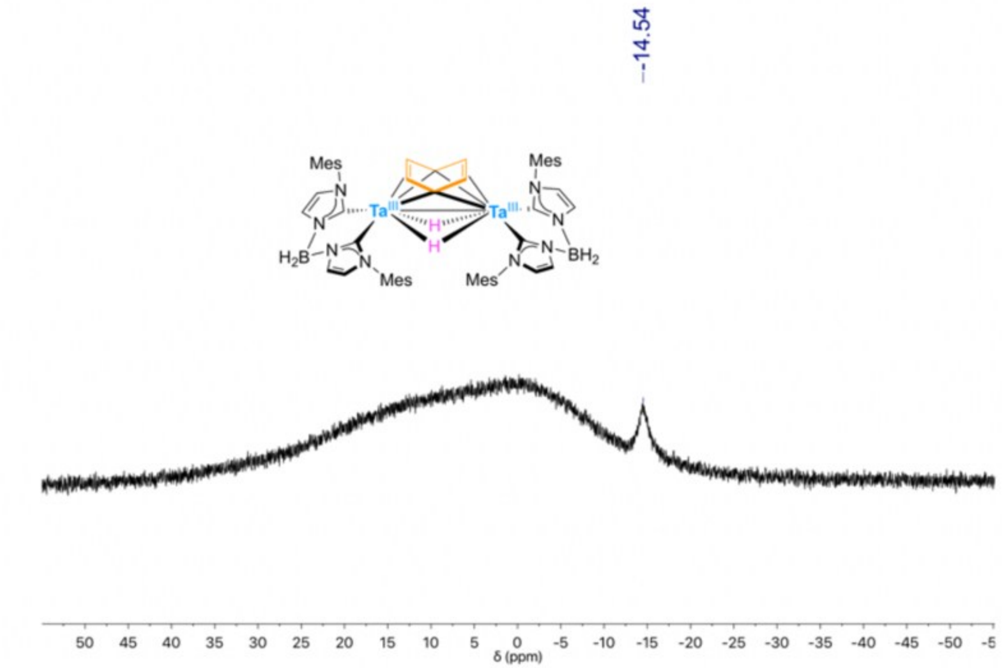

Figure S19. ^{11}B NMR spectrum of **4** in toluene-d_8 (295 K, 193 MHz). The broad resonance centered about δ 5 originates from the borosilicate glass NMR tube.

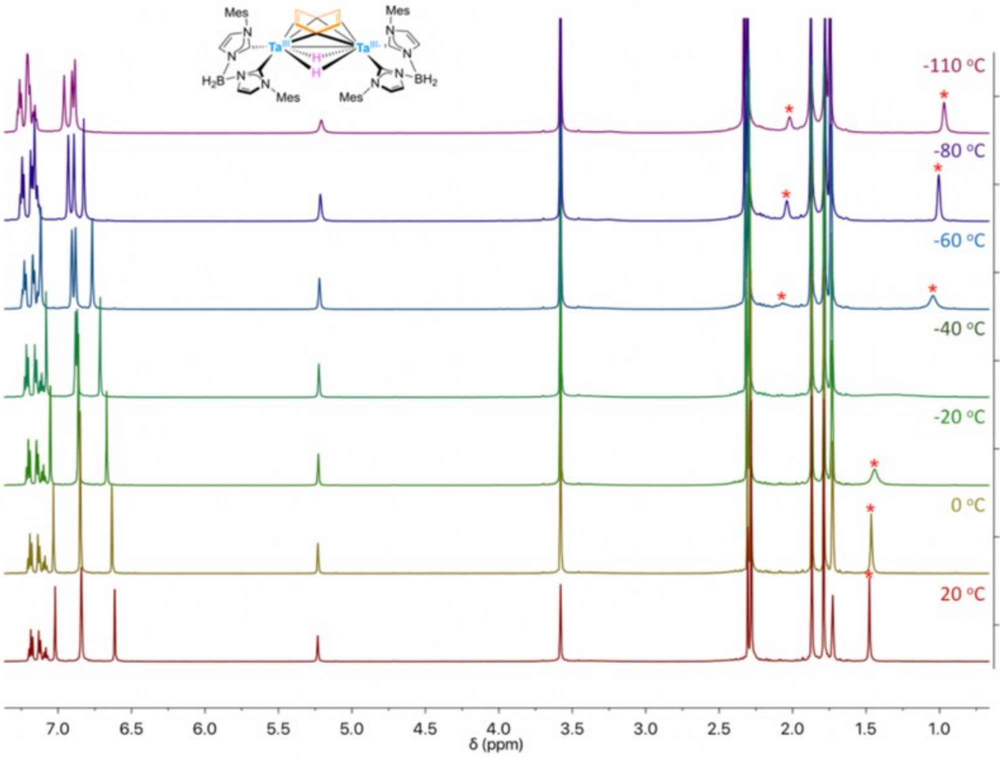

Figure S20. Variable temperature ^{1}H NMR spectra of **4** in THF-d_8 (163-293 K, 600 MHz). *The direduced benzene ligand resolves into two sharp resonances as the temperature is lowered; at –110 °C, the resonances at δ 2.02 and 0.97 integrate to two and four protons, respectively.

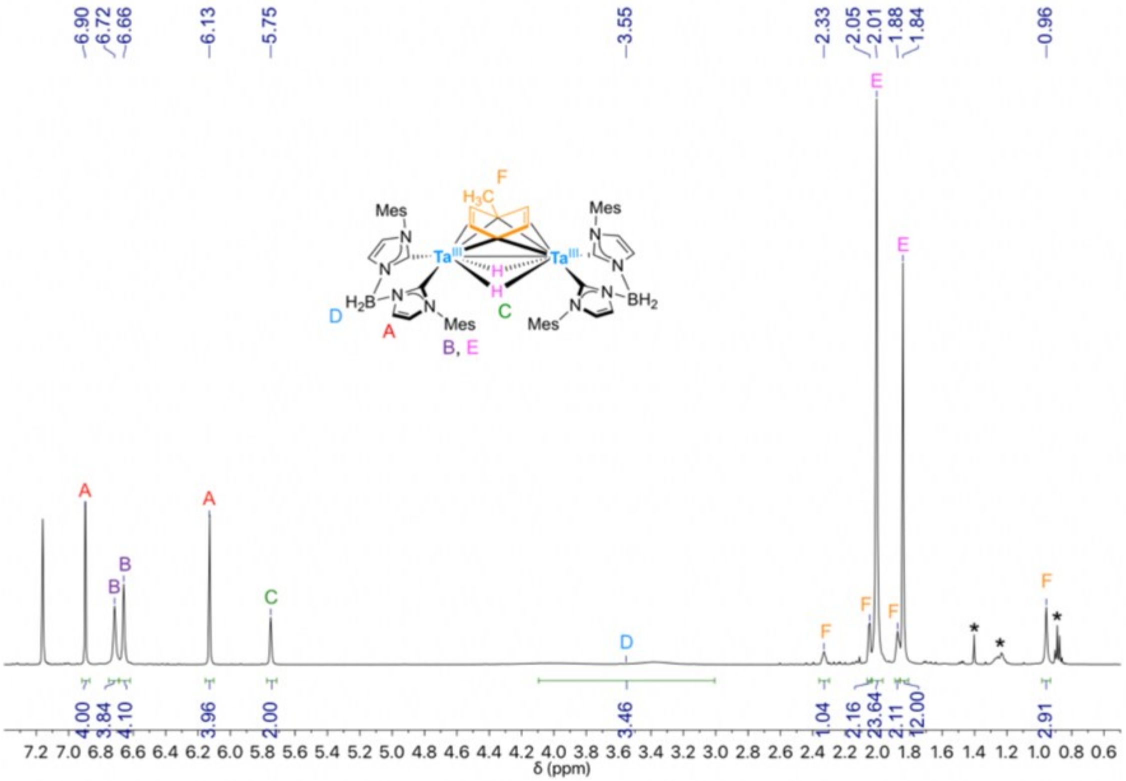

Figure S21. ^{1}H NMR spectrum of **5** in C_6D_6 (295 K, 500 MHz). *Cyclohexane and hexane.

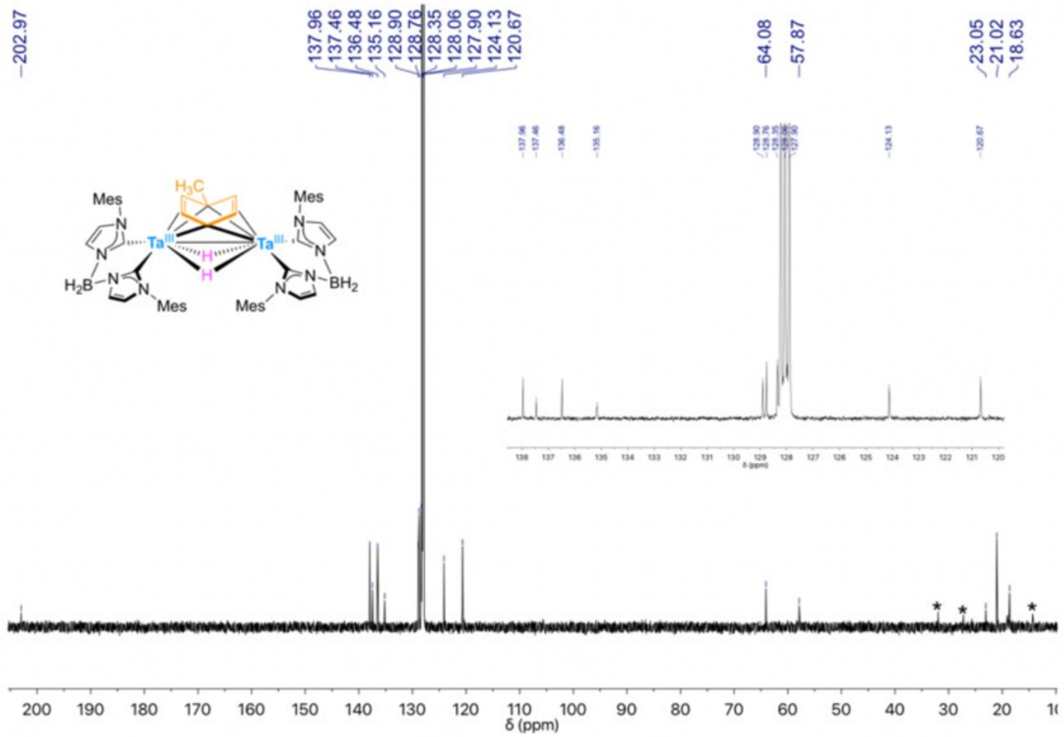

Figure S22. ^{13}C NMR spectrum of **5** in C_6D_6 (295 K, 151 MHz). *Cyclohexane and hexane.

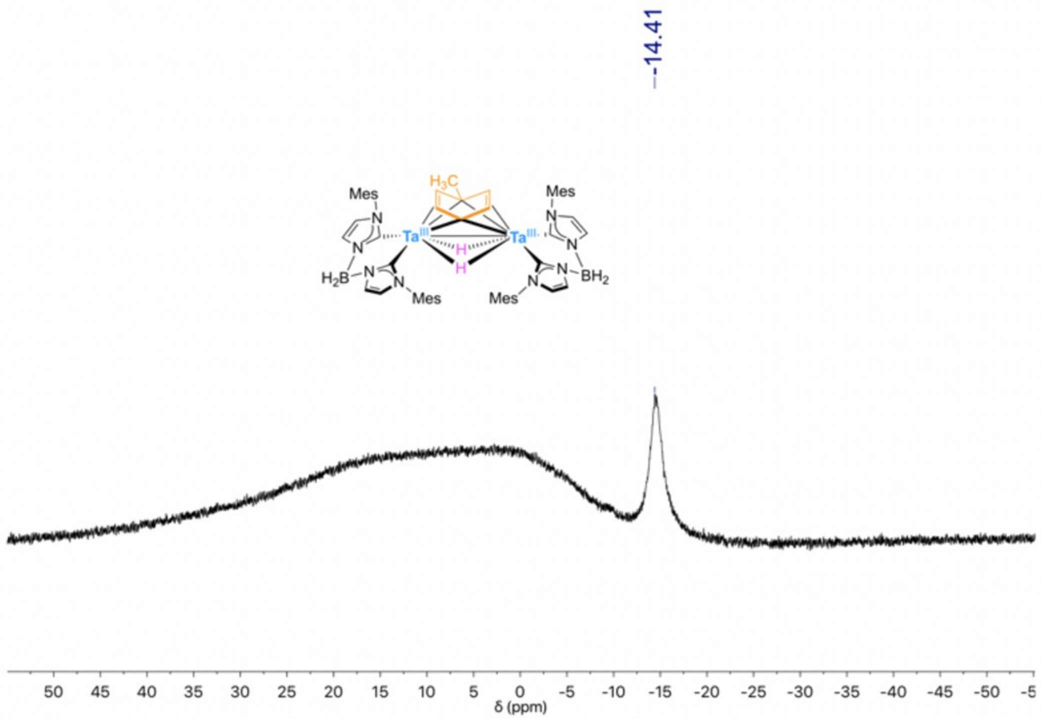

Figure S23. ^{11}B NMR spectrum of **5** in C_6D_6 (295 K, 193 MHz). The broad resonance centered about δ 5 originates from the borosilicate glass NMR tube.

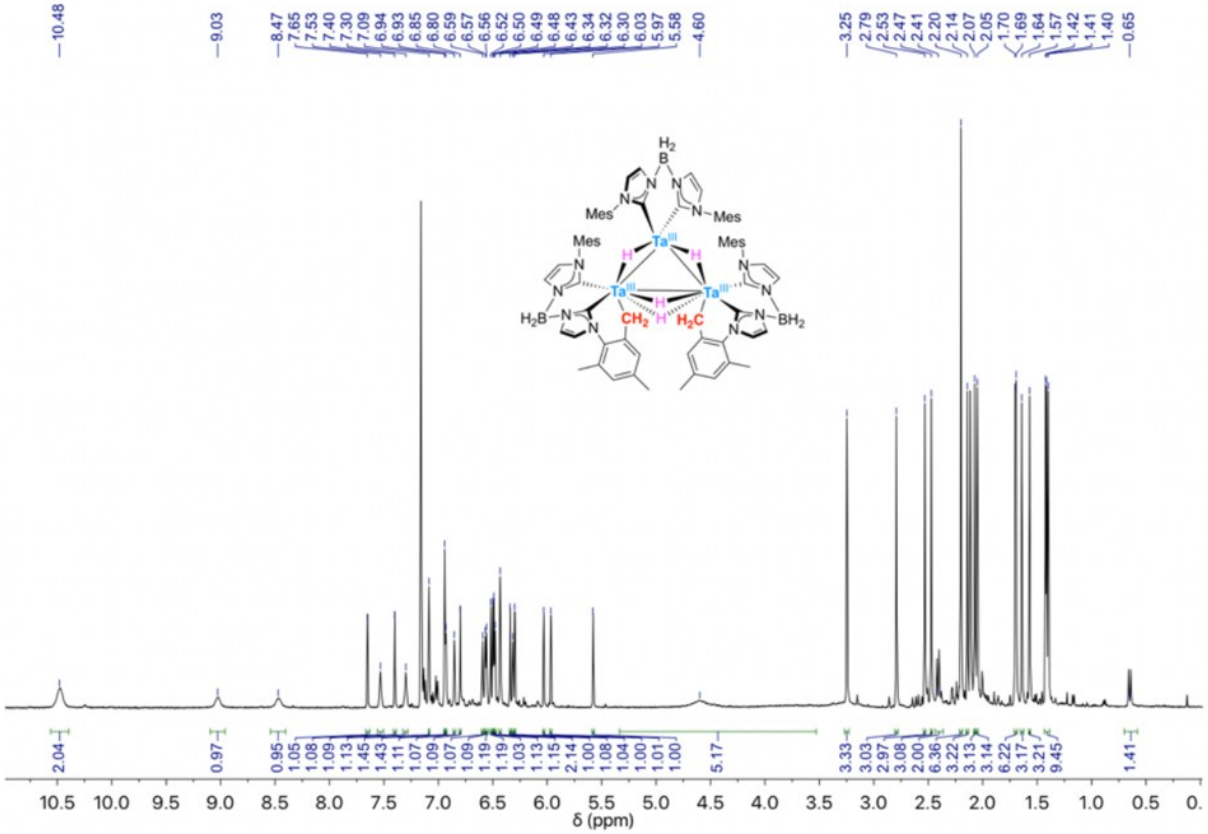

Figure S24. ^{1}H NMR spectrum of **6** C_6D_6 (295 K, 500 MHz).

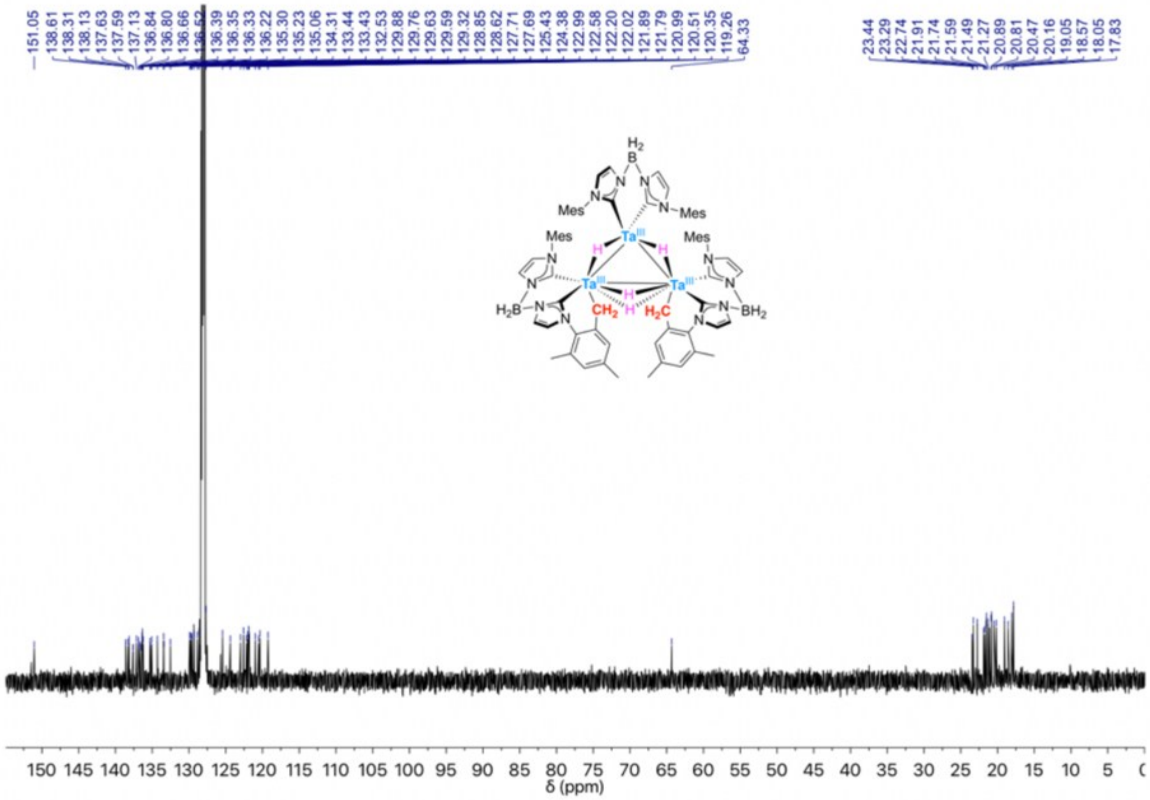

Figure S25. ^{13}C NMR spectrum of **6** in C_6D_6 (295 K, 151 MHz).

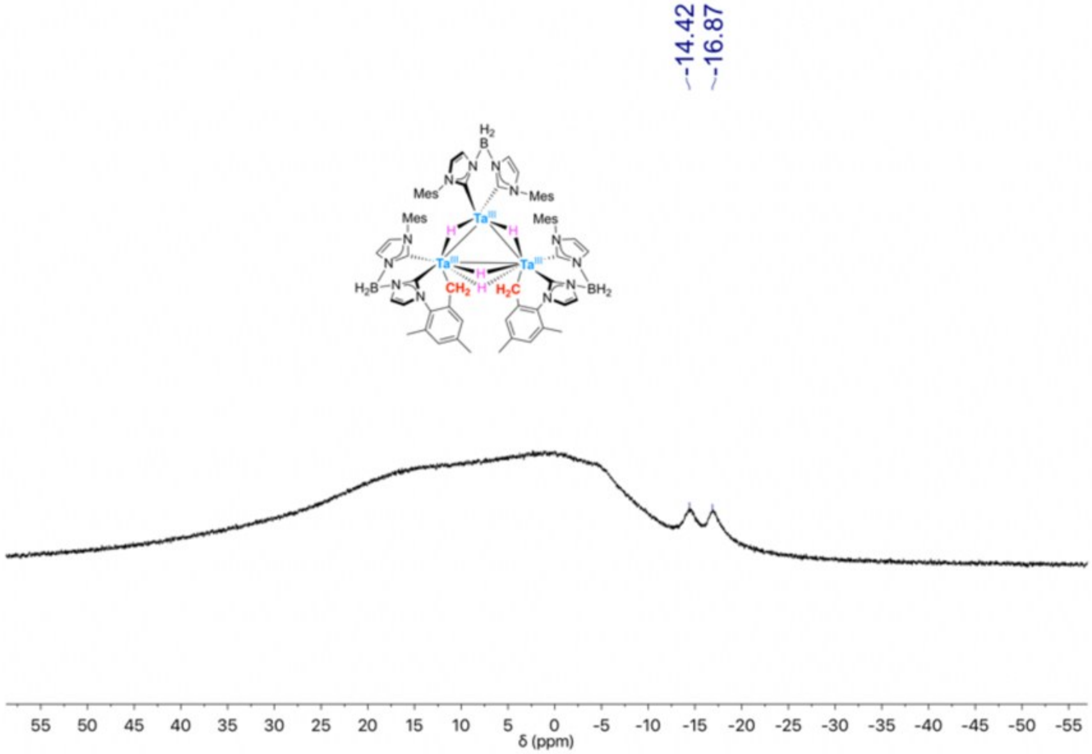

Figure S26. ^{11}B NMR spectrum of **6** in C_6D_6 (295 K, 193 MHz). The broad resonance centered about δ 5 originates from the borosilicate glass NMR tube.

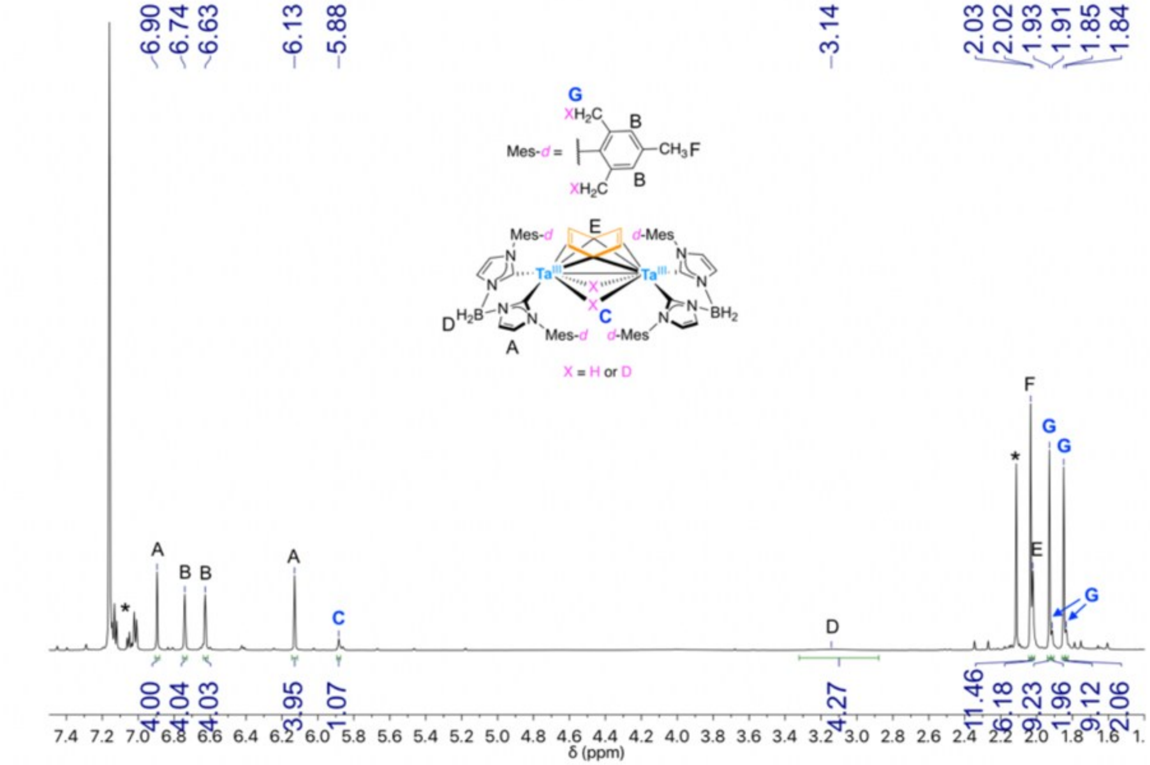

Figure S27. ^{1}H NMR spectrum of **4-*d*$_n$** C_6D_6 (295 K, 600 MHz). *Toluene.

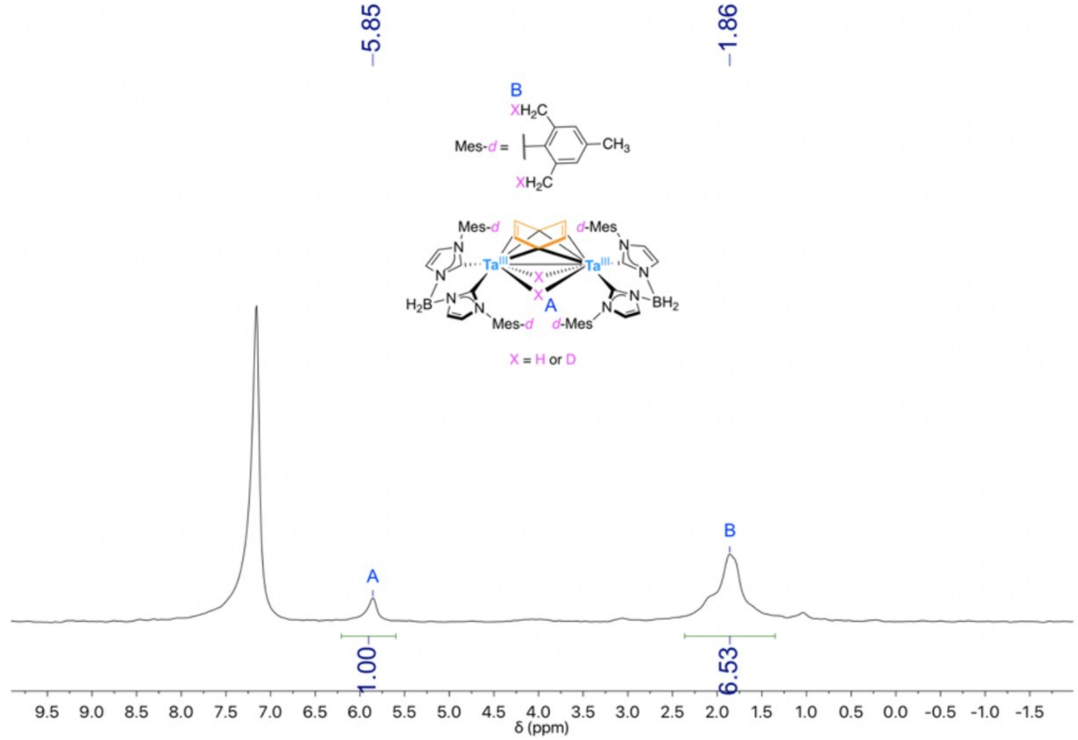

Figure S28. ^{2}H NMR spectrum of **4-*d*$_n$** C_6H_6 (295 K, 92.1 MHz).

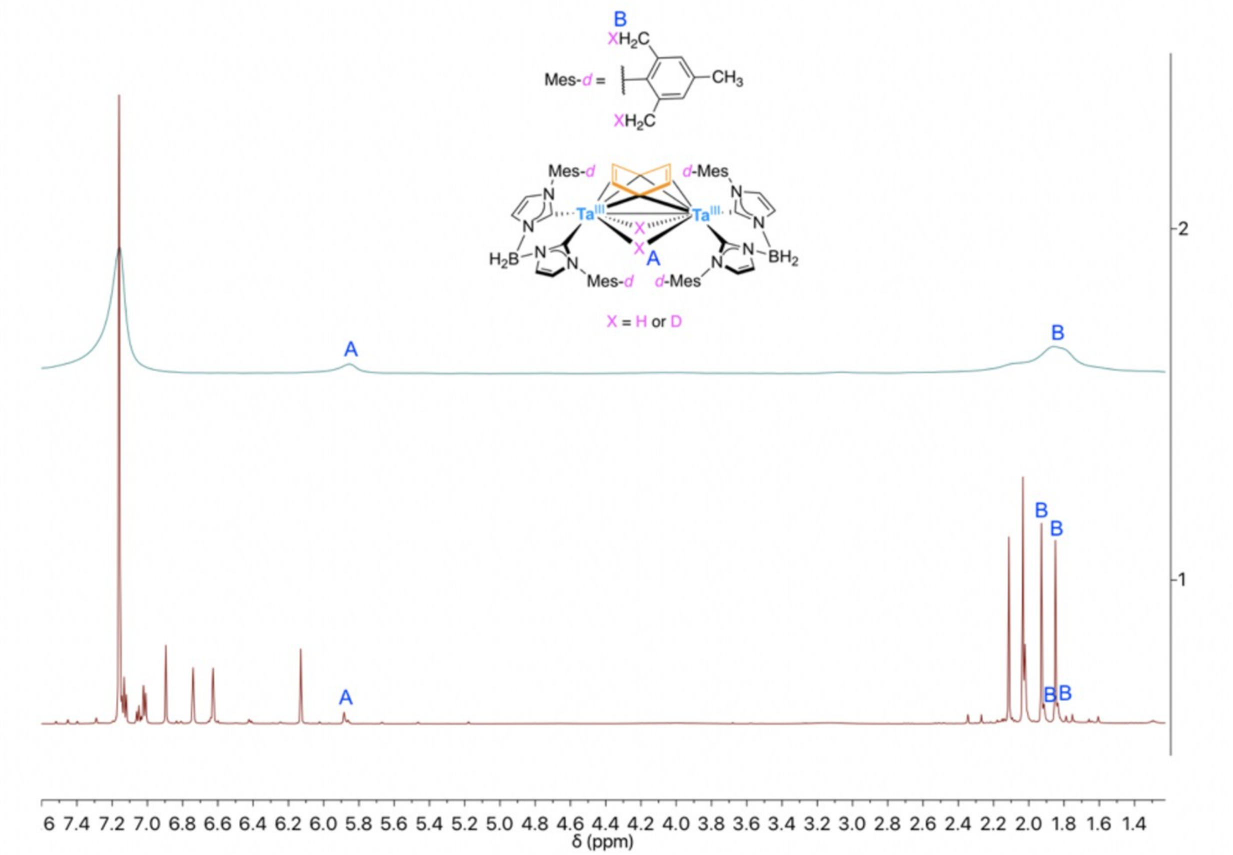

Figure S29. Overlay of ^{1}H (bottom) and ^{2}H (top) NMR spectra for **4-*d*$_\mathbf{n}$** (295 K, 600 and 92.1 MHz, respectively).

C. Crystallographic Information

X-ray crystallographic methods. X-ray structural determinations of **1**, **3**, **4**, **5**, and **7** were performed at the University of California, Berkeley, CheXray crystallographic facility. Measurements for **1**, **3**, and **4** were performed on a Rigaku XtaLAB P200 instrument equipped with a rotating-anode Mo X-ray source and a Pilatus 200K hybrid pixel array detector, and the data was analyzed, reduced, and solved using the *CrysAlis^{Pro}* software package and *Olex2* (*SHELXT* and *SHELXL*).[7] Measurements for **5** and **7** were taken using a Bruker APEX II Quazar diffractometer equipped with a micro-focus Mo X-ray source and a Bruker APEX-II CCD detector, with data analyzed and reduced using the Bruker *APEX2* software package, and solutions and refinements conducted using *Olex2* (*SHELXT* and *SHELXL*). Diffraction data for **2** and **6** were obtained at the Advanced Light Source (ALS) station 12.2.1 at Lawrence Berkeley National Laboratory, Berkeley, CA, using a silicon-monochromated beam of 17 keV (λ = 0.7288 Å) synchrotron radiation and a Bruker D8 diffractometer equipped with a Bruker PHOTON II CPAD detector. The Bruker *APEX3* software package (including *SAINT*) was used for the data collection, cell refinement, and data reduction procedures. Absorption corrections were carried out with a multiscan method using the *SADABS* program.[8] All initial structures were found using *SHELXT* and full-matrix refinements against F^2 were performed with *SHELXL-2014*.[9] All structures were collected at 100(2) K in a stream of dry nitrogen. Thermal parameters for all non-hydrogen atoms were refined anisotropically; hydrogen atoms attached to carbon atoms were included at the geometrically calculated positions and refined using a riding model. Hydrogen atoms attached to boron or tantalum atoms were located as Q peaks in the Fourier difference map and allowed to freely refine. Publication materials for **1**–**7** were made using *OLEX2*[10] and thermal ellipsoid plots were made using *Mercury*.[11] All structures were deposited to the Cambridge Crystallographic Data Centre (CCDC), with deposition numbers 1950582 (**1**), 1950578 (**2**), 1950581 (**3**), 1950580 (**4**), 1950583 (**5**), 1950579 (**6**), and 1950577 (**7**).

Table S1: Crystallographic data for compounds **1** and **2 · toluene**.

	1	**2 · toluene**
Identification code	jif002	jif007
Empirical formula	$C_{27}H_{37}BClN_4Ta$	$C_{35}H_{48}BN_4Ta$
Formula weight	644.81	716.53
Color, habit	Yellow, block	Yellow, tablet
Temperature (K)	100(2)	100(2)
Wavelength (Å)	0.71073	0.7288
Crystal system	Triclinic	Orthorhombic
Space group	P-1	$Pna2_1$
a (Å)	10.4157(3)	39.4861(15)
b (Å)	11.4099(3)	8.8759(4)
c (Å)	12.0668(2)	9.4907(4)
α (°)	93.644(2)	90
β (°)	98.974(2)	90
γ (°)	94.335(2)	90
V (Å^3)	1408.30(6)	3326.3(2)
Z	2	4
Density (Mg/m^3)	1.521	1.431
Absorption coefficient (mm^{-1})	4.019	3.528
F(000)	644.0	1456
Crystal size (mm^3)	0.18 x 0.16 x 0.10	0.13 x 0.08 x 0.02
Theta range for data collection (°)	6.858 to 59.384	2.116 to 28.331
Index ranges	$-13 \leq h \leq 13$, $-14 \leq k \leq 14$, $-14 \leq l \leq 16$	$-51 \leq h \leq 51$, $-11 \leq k \leq 11$, $-12 \leq l \leq 12$
Reflections collected	31687	35426
Independent Reflections	6830 [R(int) = 0.0411]	7676 ([R(int) = 0.0466]
Completeness	theta = 25.242°, 99.8%	theta = 25.930°, 100%
Absorption correction	Semi-empirical from equivalents	Semi-empirical from equivalents
Max. and min. transmission	1.00000 and 0.62201	0.7462 and 0.6387
Data / restraints / parameters	6830 / 0 / 316	7676 / 1 / 381
Goodness-of-fit on F^2	1.066	1.044
Final R indices [$I > 2\sigma(I)$]	$R_1 = 0.0191$, $wR_2 = 0.0455$	$R_1 = 0.0243$, $wR_2 = 0.0523$
R indices (all data)	$R_1 = 0.0209$, $wR_2 = 0.0460$	$R_1 = 0.0271$, $wR_2 = 0.0533$
Largest diff. peak and hole (e Å^{-3})	0.64 / -0.56	0.859 / -0.857

Table S2: Crystallographic data for compounds **3 · toluene** and **4**.

	3 · toluene	**4**
Identification code	jif006	jif008
Empirical formula	$C_{55}H_{68}B_2Cl_2N_8Ta_2$	$C_{54}H_{64}B_2N_8Ta_2$
Formula weight	1295.59	1208.65
Color, habit	Brown block	Blue plate
Temperature (K)	100(2)	100(2)
Wavelength (Å)	0.71073	0.71073
Crystal system	Monoclinic	Triclinic
Space group	$P2_1/c$	P-1
a (Å)	16.6448(3)	12.8612(3)
b (Å)	17.7225(4)	12.8924(3)
c (Å)	18.6699(4)	16.4689(4)
α (°)	90	86.292(2)
β (°)	96.747(2)	83.751(2)
γ (°)	90	66.080(2)
V ($Å^3$)	5469.2(2)	2480.75(12)
Z	4	2
Density (Mg/m^3)	1.573	1.618
Absorption coefficient (mm^{-1})	4.140	4.453
F(000)	2576.0	1200.0
Crystal size (mm^3)	0.20 x 0.15 x 0.06	0.41 x 0.20 x 0.05
Theta range for data collection (^{o})	6.36 to 52.744	6.224 to 52.744
Index ranges	$-20 \leq h \leq 20$, $-22 \leq k \leq 22$, $-23 \leq l \leq 23$	$-16 \leq h \leq 16$, $-16 \leq k \leq 16$, $-20 \leq l \leq 20$
Reflections collected	72862	52257
Independent Reflections	11163 [R(int) = 0.0653]	10138 [R(int) = 0.0605]
Completeness	theta = 25.000^o, 99.8%	theta = 25.242^o, 99.8%
Absorption correction	Semi-empirical from equivalents	Semi-empirical from equivalents
Max. and min. transmission	1.00000 and 0.68207	1.00000 and 0.48065
Data / restraints / parameters	11163 / 1 / 667	10138 / 0 / 639
Goodness-of-fit on F^2	1.040	1.095
Final R indices [I > 2σ(I)]	R_1 = 0.0268, wR_2 = 0.0621	R_1 = 0.0372, wR_2 = 0.0784
R indices (all data)	R_1 = 0.0357, wR_2 = 0.0654	R_1 = 0.0372, wR_2 = 0.0803
Largest diff. peak and hole (e $Å^{-3}$)	1.074 / -1.237	2.17 / -1.80

Table S3: Crystallographic data for compounds **5 · hexane** and **6 · hexane**.

	5 · hexane	**6 · hexane**
Identification code	jif011_m	jif010
Empirical formula	$C_{183}H_{240}B_6N_{24}Ta_6$	$C_{78}H_{100}B_3N_{12}Ta_3$
Formula weight	3926.54	1780.97
Color, habit	Purple prism	Purple plate
Temperature (K)	100(2)	100(2)
Wavelength (Å)	0.71073	0.7288
Crystal system	Monoclinic	Monoclinic
Space group	$P2_1/c$	P21/*n*
a (Å)	13.8721(4)	17.0723(17)
b (Å)	28.0792(8)	25.671(3)
c (Å)	44.8293(12)	17.2881(18)
α (°)	90	90
β (°)	90.941(2)	92.900(4)
γ (°)	90	90
V (Å^3)	17459.4(8)	7567.1(13)
Z	4 (Z′′ = 12)	4
Density (Mg/m^3)	1.494	1.563
Absorption coefficient (mm^{-1})	3.802	4.634
F(000)	7896.0	3544
Crystal size (mm^3)	0.25 x 0.14 x 0.20	0.09 x 0.03 x 0.01
Theta range for data collection (^{o})	1.712 to 52.746	1.864 to 26.109
Index ranges	$-17 \le h \le 17$, $-35 \le k \le 35$, $-56 \le l \le 56$	$-20 \le h \le 20$, $-30 \le k \le 30$, $-20 \le l \le 20$
Reflections collected	278605	102483
Independent Reflections	35701 [R(int) = 0.0742]	13925 [R(int) = 0.0713]
Completeness	theta = 25.242^o, 100%	theta = 26.930^o, 100%
Absorption correction	Semi-empirical from equivalents	Semi-empirical from equivalents
Max. and min. transmission	0.7457 and 0.5793	0.7453 and 0.5849
Data / restraints / parameters	35701 / 0 / 2125	13925 / 38 / 899
Goodness-of-fit on F^2	1.058	1.042
Final R indices [I > 2σ(I)]	$R_1 = 0.0369$, $wR_2 = 0.0620$	$R_1 = 0.0343$, $wR_2 = 0.0834$
R indices (all data)	$R_1 = 0.0521$, $wR_2 = 0.0660$	$R_1 = 0.0470$, $wR_2 = 0.0891$
Largest diff. peak and hole (e Å^{-3})	1.13 / -1.24	3.247 / -1.329

Table S4: Crystallographic data for compound **7**.

	7
Identification code	jif009
Empirical formula	$C_{72}H_{88}B_3N_{12}Ta_3$
Formula weight	1696.82
Color, habit	Purple needle
Temperature (K)	100(2)
Wavelength (Å)	0.71073
Crystal system	Monoclinic
Space group	$P2_1/n$
a (Å)	20.5383(9)
b (Å)	12.5927(5)
c (Å)	33.4495(14)
α (°)	90
β (°)	106.533(2)
γ (°)	90
V (Å^3)	8293.5(6)
Z	4
Density (Mg/m^3)	1.359
Absorption coefficient (mm^{-1})	3.991
F(000)	3352.0
Crystal size (mm^3)	0.04 x 0.01 x 0.01
Theta range for data collection (^{o})	2.54 to 50.882
Index ranges	$-24 \leq h \leq 24$, $-13 \leq k \leq 15$, $-40 \leq l \leq 40$
Reflections collected	80563
Independent Reflections	15306 [R(int) = 0.1250]
Completeness	theta = 25.242^o, 100%
Absorption correction	Semi-empirical from equivalents
Max. and min. transmission	0.7452 and 0.6059
Data / restraints / parameters	15306 / 3 / 865
Goodness-of-fit on F^2	1.012
Final R indices [I > 2σ(I)]	$R_1 = 0.0566$, $wR_2 = 0.0912$
R indices (all data)	$R_1 = 0.0935$, $wR_2 = 0.1011$
Largest diff. peak and hole (e Å^{-3})	1.87 / -1.21

Table S5: Selected bond lengths (Å) for **1** and **2 · toluene**.

Bond	**1**	**2 · toluene**
Ta – Me (range)	2.178(2) – 2.198(2)	2.177(5) – 2.200(6)
Ta – $C_{Carbene}$	2.293(2), 2.305(2)	2.315(5), 2.327(5)
Ta – Cl	2.3927(6)	N/A

Table S6: Selected bond lengths (Å) for **3 · toluene**.

Bond	**3 · toluene**
Ta – Ta	2.5594(5)
Ta – $C_{Carbene}$ (range)	2.238(3) – 2.255(3)
Ta – Cl	2.3309(9), 2.3351(9)
Ta – H (range)	1.66(4) – 2.05(3)

Table S7: Selected bond lengths (Å) and torsion angles (°) for **4** and **5 · hexane**.

Bond/angle	**4**	**5 · hexane** (Z = 4, Z″ = 12)
Ta – Ta	2.6328(4)	2.6138(6) – 2.6191(6) (range)
Ta – $C_{Carbene}$ (range)	2.268(3) – 2.280(3)	2.262(4) – 2.315(4)
Ta – H (range)	1.81(4) – 1.92(4)	1.79(4) – 1.96(6)
Arene C – C (range)	1.426(5) – 1.446(6)	1.415(7) – 1.452(6)
Arene torsion (range)	21.2(3) – 23.0(3)	18.4(3) – 19.8(3)

Table S8: Selected bond lengths (Å) for **6 · hexane** and **7**.

Bond	**6 · hexane**	**7**
Ta – Ta (range)	2.6334(7) – 2.8974(7)	2.6265(7) – 2.8839(6)
Ta – $C_{Carbene}$ (range)	2.228(5) – 2.395(5)	2.221(9) – 2.342(8)
Ta – H (range)	1.74(5) – 1.98(5)	1.51(6) – 1.92(6)
Ta – CH_2	2.254(5), 2.291(5)	2.273(9)

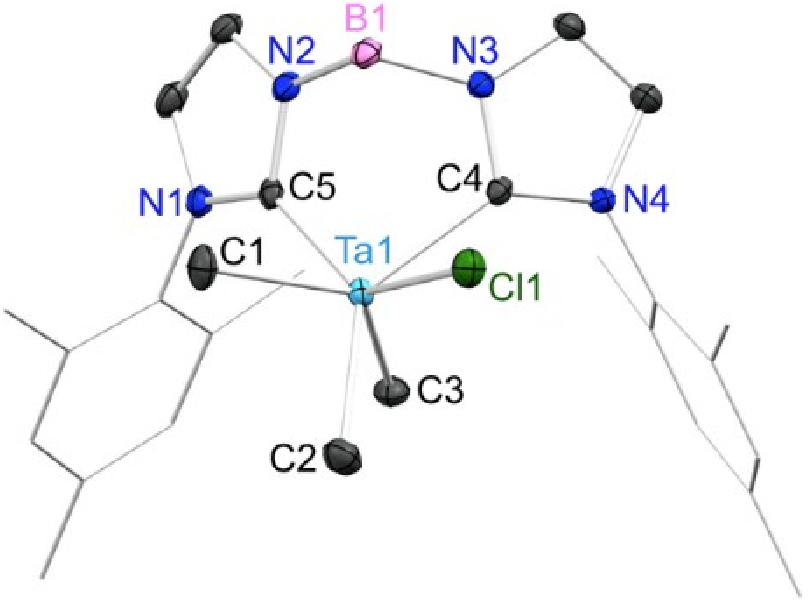

Figure S30. Crystal structure of **1** with 50% probability thermal ellipsoids. H atoms are excluded, and mesityl groups are depicted in wireframe for clarity.

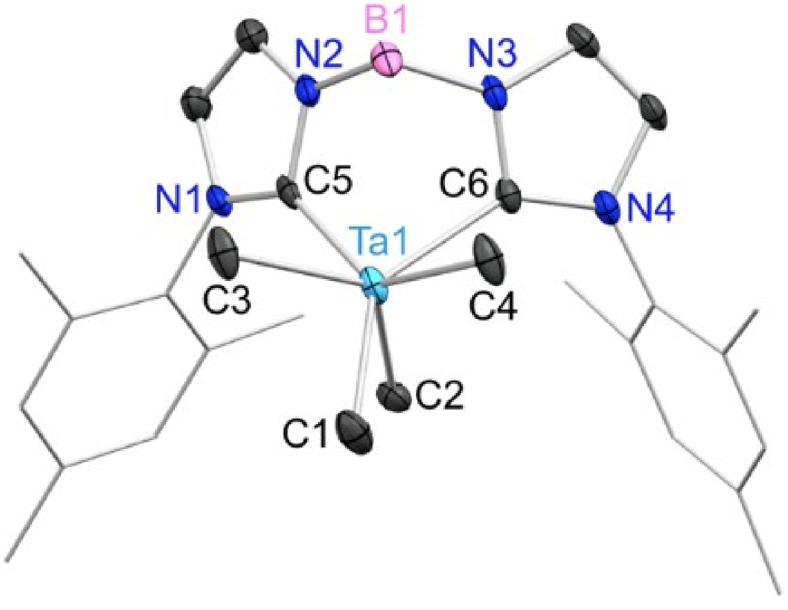

Figure S31. Crystal structure of **2** with 50% probability thermal ellipsoids. H atoms and lattice solvent are excluded, and mesityl groups are depicted in wireframe for clarity.

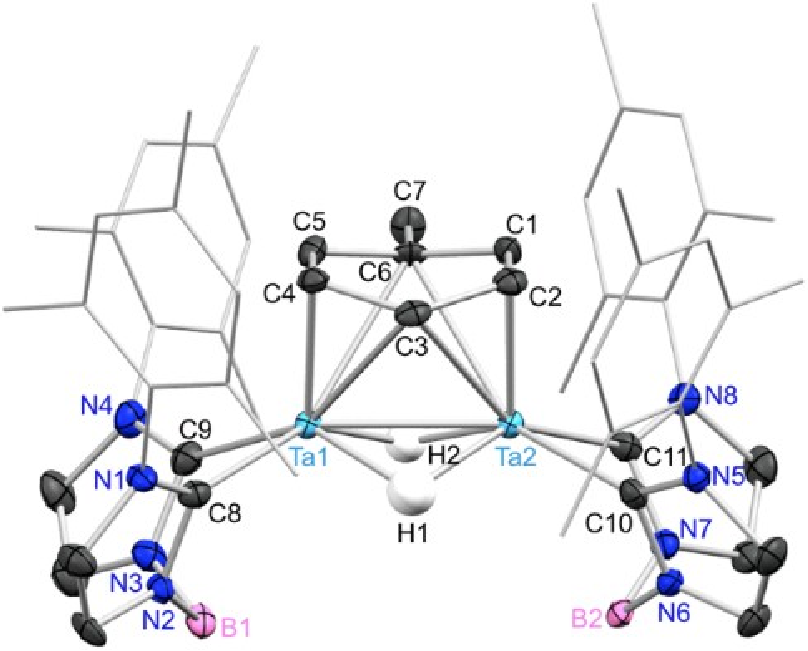

Figure S32. Crystal structure of **5** with 50% probability thermal ellipsoids. H atoms (except the bridging hydrides) and lattice solvent are excluded, and mesityl groups are depicted in wireframe for clarity.

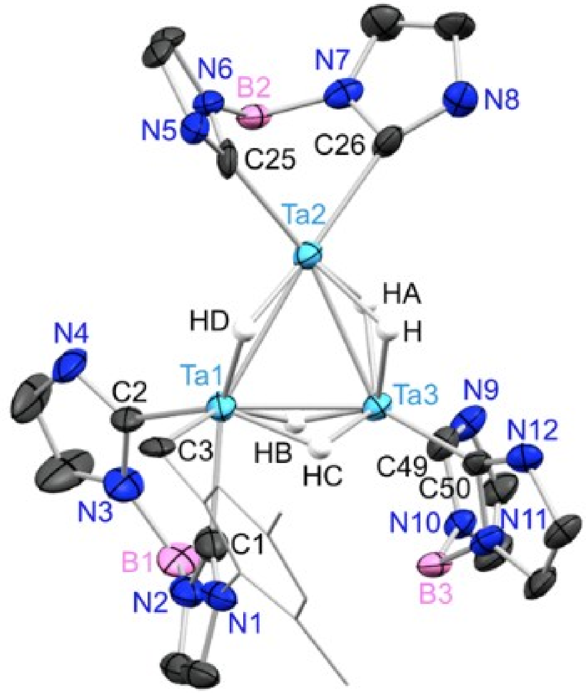

Figure S33. Crystal structure of **7** with 50% probability thermal ellipsoids. H atoms (except the bridging hydrides) and mesityl groups (except the cyclometallated group, which is depicted in wireframe) are excluded for clarity. Disordered lattice solvent was treated with the BYPASS routine included in the OLEX2 software package.[12]

D. Computational Details

Computational methods. Calculations were carried out with the *Gaussian16* program,[13] employing the wB97XD functional with standard 6-31G‡(d,p) basis set for C, H, B, and N[14] and Stuttgart-Dresden RECP (relativistic effective core potential) basis set with 28 core electrons for Ta,[15] to fully optimize the geometry of the complex (with no symmetry restrictions imposed). All resultant stationary points were characterized by vibrational analyses as local minima without imaginary frequencies. For computational efficiency, calculations were carried out on truncated versions of the complexes of interest, in which the mesityl substituents were replaced with phenyl groups (Figure S30). Coordinates of optimized structures can be found as .mol2 files within the supplementary .zip file associated with this publication.

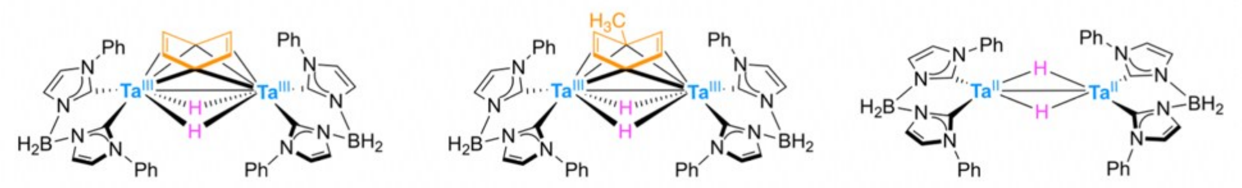

$\mathbf{4^{Ph}}$ $\mathbf{5^{Ph}}$ $\mathbf{A^{Ph}}$

Figure S34. DFT-optimized structures and corresponding abbreviations.

Table S9: Energies of DFT-optimized structures and calculated energy of arene binding.

Molecule(s) of Interest	Energy (Hartrees)	Energy (kcal/mol)
$\{[H_2B(^{Ph}Im)_2]Ta\}_2(\mu\text{-}H)_2(\mu\text{-}\eta^4{:}\eta^4\text{-}C_6H_6)$ ($\mathbf{4^{Ph}}$)	-2225.903884	-1396776.1
$\{[H_2B(^{Ph}Im)_2]Ta\}_2(\mu\text{-}H)_2(\mu\text{-}\eta^4{:}\eta^4\text{-}C_7H_8)$ ($\mathbf{5^{Ph}}$)	-2265.209328	-1421440.6
$\{[H_2B(^{Ph}Im)_2]Ta\}_2(\mu\text{-}H)_2$ ($\mathbf{A^{Ph}}$)	-1993.623672	-1251018.0
C_6H_6	-232.180850	-145695.7
C_7H_8	-271.490303	-170362.8
$\mathbf{A^{Ph}}$ + C_6H_6	-2225.804522	-1396713.7
$\mathbf{A^{Ph}}$ + C_7H_8	-2265.113975	-1421380.8
C_6H_6 binding interaction [$\mathbf{4^{Ph}}$ – ($\mathbf{A^{Ph}}$ + C_6H_6)]	-0.099362	-62.4
C_7H_8 binding interaction [$\mathbf{5^{Ph}}$ – ($\mathbf{A^{Ph}}$ + C_7H_8)]	-0.095353	-59.8

Table S10: Comparison of selected bond lengths (Å) and torsion angles (°) for crystal structure **4** and DFT-optimized structure **4^{Ph}**.

Bond/angle	Crystal structure **4**	DFT-optimized structure **4^{Ph}**
Ta – Ta	2.63266(7)	2.59525
Ta – $C_{Carbene}$ (range)	2.26722(8) – 2.28032(8)	2.28922 – 2.31938
Ta – H (range)	1.81489(4) – 1.92051(4)	1.91186 – 1.93896
Arene C – C (range)	1.42597(4) – 1.44621(3)	1.43418 – 1.45670
Arene torsion (range)	21.1876(7) – 22.9645(10)	20.63550 – 21.48097

Table S11: Comparison of selected bond lengths (Å) and torsion angles (°) for crystal structure **5 · hexane** and DFT-optimized structure **5^{Ph}**.

Bond/angle	Crystal structure **5 · hexane**	DFT-optimized structure **5^{Ph}**
Ta – Ta	2.61393(5) – 2.61929(5) (range)	2.59964
Ta – $C_{Carbene}$ (range)	2.262(4) – 2.2315(4)	2.29745 – 2.34445
Ta – H (range)	1.79(4) – 1.96(6)	1.89099 – 1.96442
Arene C – C (range)	1.41584(4) – 1.45240(3)	1.42176 – 1.46891
Arene torsion (range)	18.4188(7) – 19.8186(7)	18.19144 – 20.14370

E. References

1 G. Occhipinti, V. R. Jensen, K. W. Törnroos, N. Å. Frøystein, and H.-R. Bjørsvik, *Tetrahedron*, 2009, **65**, 7186.

2 M. E. Garner, S. Hohloch, L. Maron, and J. Arnold, *Organometallics*, 2016, **35**, 2915.

3 J. A. Ziegler, C. Prange, T. D. Lohrey, R. G. Bergman, and J. Arnold, *Inorg. Chem.*, 2018, **57**, 5213.

4 R. Neufeld, M. John, and D. Stalke, *Angew. Chem., Int. Ed.*, 2015, **54**, 6994.

5 R. R. Schrock and P. R. Sharp, *J. Am. Chem. Soc.*, 1978, **100**, 2389.

6 M. A. Araya, F. A. Cotton, J. H. Matonic, and C. A. Murillo, *Inorg. Chem.*, 1995, **34**, 5424.

7 Rigaku Oxford Diffraction, 2015, CrysAlisPro Software system, version 1.171.39.7a, Rigaku Coroporation, Oxford, UK.

8 *SADABS: Bruker-Nonius Area Detector Scaling and Absorpton;* Bruker Analytical X-ray Systems, Inc., Madison, WI, 2003.

9 G. M. Sheldrick, *Acta Crystallogr., Sect. A: Found. Crystallogr.*, 2008, **64**, 112.

10 O. V. Dolomanov, L. J. Bourhis, R. J. Gildea, J. A. K. Howard, and H. Puschmann, *J. Appl. Crystallogr.*, 2009, **42**, 339.

11 C. F. Macrae, I. J. Bruno, J. A. Chisholm, P. R. Edgington, P. McCabe, E. Pidcoc, L. Rodriguez-Monge, R. Taylor, J. Van De Streek, and P. A. Wood, *J. Appl. Crystallogr.*, 2008, **41**, 466.

12 P. Van der Sluis and A. L. Spek, *Acta Cryst.*, 1990, **A46**, 194.

13 M. J. Frisch, G. W. Trucks, H. B. Schlegel, G. E. Scuseria, M. A. Robb, J. R. Cheeseman, G. Scalmani, V. Barone, B. Mennucci, G. A. Petersson, H. Nakatsuji, M. Caricato, X. Li, H. P. Hratchian, A. F. Izmaylov, J. Bloino, G. Zheng, J. L. Sonnenberg, M. Hada, M. Ehara, K. Toyota, R. Fukuda, J. Hasegawa, M. Ishida, T. Nakajima, Y. Honda, O. Kitao, H. Nakai, T. Vreven, J. A. Montgomery, Jr., J. E. Peralta, F. Ogliaro, M. Bearpark, J. J. Heyd, E. Brothers, K. N. Kudin, V. N. Staroverov, T. Keith, R. Kobayashi, J. Normand, K. Raghavachari, A. Rendell, J. C. Burant, S. S. Iyengar, J. Tomasi, M. Cossi, N. Rega, J. M. Millam, M. Klene, J. E. Knox, J. B. Cross, V. Bakken, C. Adamo, J. Jaramillo, R. Gomperts, R. E. Stratmann, O. Yazyev, A. J. Austin, R. Cammi, C. Pomelli, J. W. Ochterski, R. L. Martin, K. Morokuma, V. G. Zakrzewski, G. A. Voth, P. Salvador, J. J. Dannenberg, S. Dapprich, A. D. Daniels, O. Farkas, J. B. Foresman, J. V. Ortiz, J. Cioslowski, and D. J. Fox, Gaussian, Inc., Wallingford CT, 2016.

14 G. A. Petersson and M. A. Al-Laham, *J. Chem. Phys.*, 1991, **94**, 6081.

15 D. Andrae, U. Haeussermann, M. Dolg, H. Stoll, and H. Preuss, *Theor. Chem. Acc.*, 1990, **77**, 123.